ELSEVIER

Catalysis Today 27 (1996) 403–435

CATALYSIS TODAY

IR studies of CO and NO adsorbed on well characterized oxide single microcrystals

Adriano Zecchina [a,*], Domenica Scarano [a], Silvia Bordiga [a], Gabriele Ricchiardi [a], Giuseppe Spoto [a], Francesco Geobaldo [b]

[a] *Dipartimento di Chimica Inorganica, Chimica Fisica e Chimica dei Materiali, Università di Torino, Via Pietro Giuria 7, 10125 Turin, Italy*

[b] *Dipartimento di Scienza dei Materiali e Ingegneria Chimica, Politecnico di Torino, Corso Duca degli Abruzzi 24, 10123 Turin, Italy*

Abstract

A systematic investigation of the surface morphology and of the vibrational properties of CO and NO adsorbed on simple oxides microcrystals (like MgO, NiO, NiO–MgO, CoO–MgO, ZnO, ZnO–CoO, α-Cr_2O_3, α-Al_2O_3, $MgAl_2O_4$ and other spinels, TiO_2, ZrO_2 and other oxides of a similar structure) with regular crystalline habit and exposing thermodynamically stable and neutral faces, is presented with the aim to elucidate the spectroscopic manifestations of CO and NO adsorbed on well defined crystallographic positions.

In particular the structure of CO and NO adsorbed on the cationic sites of extended faces of these model solids is presented and discussed with the aim of elucidating the nature of the $Me^{x+} \cdots CO/NO$ bond (Me^{x+} = non transition metal ion or transition metal ion). When non transition metal ions are involved, the molecule–cation interaction is predominantly electrostatic. This leads to an increase of the CO stretching frequency, which is roughly proportional to the polarizing field. On the contrary, when transition metal ions are involved, beside the predominant electrostatic interactions, a small contribution to the bond stability comes also from d–π overlap forces, which, although not very important from the energetic point of view, greatly influence the static and dynamic dipoles localized on the adsorbed molecules. Consequently, the strength of the dipole–dipole interactions occurring in the ordered adlayers of CO and NO adsorbed on transition and non transition metal oxide surfaces are resulted remarkably different.

On these well defined surfaces, the effects influencing the half-width (FWHM) of the CO and NO stretching peaks have also been considered. It has been calculated that the FWHM is a very sensitive parameter of the surface perfection. In a few cases (ZnO, α-Cr_2O_3, etc.) FWHM values comprised in the 1.5–3.7 range have been obtained, which are indicative of a single-crystal quality of the exposed faces. These spectroscopic results were compared with those obtained with quantum calculations.

Finally the activity towards CO and NO of perfect, low index faces and of more defective situations (like those associated with edges, steps and corners) are compared, in order to have a better insight on the role of surface defectivity in catalytic reactions.

Keywords: Infrared spectrometry; Carbon monoxide; Nitrogen oxide; Microcrystals of oxides

1. Introduction

Although oxides are certainly representing one of the most important and widely employed classes of solids (as catalyst and catalytic sup-

* Corresponding author.

SSDI 0920-5861(95)00202-2

ports and in the form of films for various applications in several branches of the material science), the studies of their surface properties with the classical methods of the surface science applied to well defined single crystals surfaces are scarcely developed. This situation is associated with the additional difficulties which are encountered in this type of studies, owing to the insulating character of many of these solids preventing (unlike metals and semiconductors [1–10]) the wide application of classical surface science electron spectroscopies (like high resolution electron energy-loss spectroscopy (HREELS) and others) to the study of the structure of the adsorbed overlayers.

The lack of data on model oxide systems is particularly relevant when catalytic surfaces are considered, not only because the oxides possess catalytic properties of their own or participate as supports to many metal–catalyzed reactions, but also because it is becoming gradually more and more clear that reactions which are universally considered as metal–catalyzed reactions (for instance the Fisher–Tropsh reaction, ammonia synthesis and dehydrosulfurization reactions) do actually occur on surfaces variously carbided, oxidized, nitrided and sulphided (and more in general functionalized) because of the presence of reactants and products. As a consequence, also in this case, the detailed knowledge of the surface properties of reference oxides (but also of nitrides, sulphides and carbides as well) could be of great help in the understanding of the basic catalytic phenomena and mechanisms.

While the studies on well defined (single crystals) oxide surfaces are not well developed, the studies on dispersed materials, on the contrary, have received much attention because of their very evident and direct relevance in catalysis and of the easy applicability of simple physical methods (like for instance IR and UV–vis., both in transmission and reflectance configuration, Raman, EPR and NMR spectroscopies). The contributions in this field are very numerous and several reviews have been published to illustrate the constant progress in this area [11–30]. However these studies (like the similar ones on dispersed metals) suffer a very evident limitation as they are conducted on poorly defined systems: they do in fact give only integrated information on the properties of a great variety of surface species (simultaneously formed on the different surface sites necessarily present on high surface area systems). As the spectroscopic manifestations of these different species are often superimposed, the interpretation of the spectra and the attribution of the spectroscopically separated components (when present) is often difficult or even impossible and rarely free of ambiguities.

From these considerations the importance of surface science studies on well defined oxidic systems (to act as indispensable milestones for the full comprehension of the data obtained on dispersed materials) should be clearly emerging.

Well defined surfaces can, in principle, be obtained in three different ways: (i) by cutting a macroscopic crystal along a well defined plane; (ii) by epitaxial growth of ordered oxide films on top of (macroscopic) single crystal metal faces; (iii) by preparing microcrystals of well defined morphology exposing only a few defect-free extended faces.

Only a very few investigations based on route (i) have been reported [31–33]. It is worth noticing that the vibrational spectra of species formed on single crystal surfaces prepared in this way cannot be easily obtained in reflection mode (RAIRS) and transmission experiments have proved to be more appropriate: see for instance Refs. [34,35], where high band resolution conditions (≤ 1 cm^{-1}) were easily achieved. Notice that charging problems imposes severe limitations to the use of HREELS methods so common in metals surface science. Moreover, in all cases (except alkali halides) oxide surfaces not directly cut in vacuo in the measurement apparatus, can only be cleaned with difficulty from dissociatively adsorbed water. All together, these facts probably explain the paucity of the experimental data so far produced.

As far as the second route is concerned, the data produced so far are slightly more abundant (see for instance Refs. [36–53]) and presumably will increase strongly in the future, since there are no limitations in the combined and synergic use of electron spectroscopies (like UPS, ARUPS and in particular of HREELS) and of structural methods like LEED. In principle this method can allow the epitaxial growth of any type of surface plane, even those not electrically neutral and so very reactive and thermodynamically unstable. One possible drawback of these techniques lies in the incomplete control of the number of surface defects which are present in these ultrathin films.

The third route is based on the documented observation that, when proper synthesis and sintering conditions are adopted, oxides microparticles of a dispersed material (generally with dimensions of 100–200 nm and specific surface area ≤ 10 m^2 g^{-1}) can assume the crystalline habit of very regular and perfect polyhedra exposing few, thermodynamically stable and hence neutral faces. As the scattering properties of these samples are, in general, not prohibitive, high resolution IR spectroscopy in the transmission mode can be easily performed with modern FTIR instruments, on pelleted samples inside suitable cells, which allow high temperature treatments under high vacuo to be performed. The spectra of the surface species observed on these types of systems (carried out at any $T \geq$ 77K) can be very simple and of unambiguous interpretation and the intensity of the peaks is generally strong or very strong (even on materials with a specific surface area of ca. 1 m^2 g^{-1}). The interpretation of the vibrational modes of surface species hence becomes feasible and accurate. However, as even on lowest surface area materials the number of surface sites located at the borders of the facelets (and, to a lower extent, on edges and corners) is not negligible, the spectra can be slightly more complicated than those characteristic of the infinite faces. Moreover, as in only a few cases involving cubic solids do the microcrystals polyhedra terminate with a single type of crystallographic plane, the IR spectrum is necessarily due to the superposition of the bands of more than one type of surface species: this definitely represents a limitation. Of course, to be productive, the method requires an adequate analysis of the microcrystals morphology through the combined use of high resolution electron microscopy (HRTEM), electron diffraction and computer graphics. Often, other types of microscopies are needed like scanning electron microscopy or atomic force microscopy (especially when the particles dimensions are so large as to prevent any measurement in the transmission mode). Let us remark that one advantage of the method lies in the possibility (by using appropriate sintering procedures) of virtually preparing samples with any type of surface area varying from the values typical of the real catalysts to those more typical of single microcrystals. In this way the whole range of highly disordered, very reactive and catalytically useful surfaces and the reference low index faces of the single crystals can be covered, so contributing the establishment of a link between the studies conducted on catalytic materials and the studies on single crystals with surface science methods. The progressive sintering route has been followed in our laboratory for many years and the IR spectra of simple molecules adsorbed on several oxidic systems have been interpreted. As in Chapter 1 of this book an introduction to the vibrational spectroscopies applied to metal oxide catalysts is presented and as the application of vibrational spectroscopies to real oxides catalysts is exemplified in Chapter 8, in this Chapter no effort will be made to illustrate the fundamental aspects of the IR spectroscopy application to surface studies.

In this review we shall mainly describe the IR spectra of CO and NO adsorbed on simple oxides microcrystals like MgO [54–57], NiO [58–63], NiO–MgO [64–70], CoO–MgO [66,71–74], ZnO [75–79], ZnO–CoO [80], α-Cr_2O_3 [81–86] and α-Al_2O_3 [87], $MgAl_2O_4$ and other spinels [88,89], TiO_2 [90–92], ZrO_2

[93,94] and other oxides with a similar structure. When possible, these results will be compared with those obtained with other methods and with the results of quantum calculations.

2. Oxides with a cubic (rock-salt) structure (MgO, NiO, MgO–NiO and MgO–CoO)

2.1. The IR spectroscopy of the MgO–CO system

MgO, NiO and their solid solutions, having the same crystalline (rock-salt) structure, similar lattice parameter (ca. 0.29 nm) and similar cubic habit, represent an ideal family of solids to start the illustration of the method of progressive sintering and to show its utility in surface science studies. Within this range, MgO is particularly useful since its morphology changes upon thermal treatments, having been studied in our laboratory in the past by means of electron microscopy [56,57,66], are perfectly known. For this reason the illustration of the modifications of the surface properties of this oxide upon increasing the dimension and the perfection of the microcrystals represents an ideal example.

High surface area MgO is usually prepared by decomposition of brucite $Mg(OH)_2$ at 520–550 K in vacuo. The hexagonal platelets of brucite are topotactically transformed into aggregates of cubelets exposing preferentially [100] faces, as it is schematically drawn in Fig. 1.

The average edge length of these cubelets is ca. 7 nm (in agreement with the high value of the surface area: 200 $m^2\ g^{-1}$): this means that the area of the cubic facelets is ca. 50 nm^2. It has been calculated [66] that on this type of systems the percentage of surface atoms (either Mg or O) in corner, edge and face position is ca. 1%, ca. 15% and ca. 84%, respectively, which is indeed very far from an infinite and perfect single crystal [100] face. Once formed at 520–550 K, the surface is fully covered by

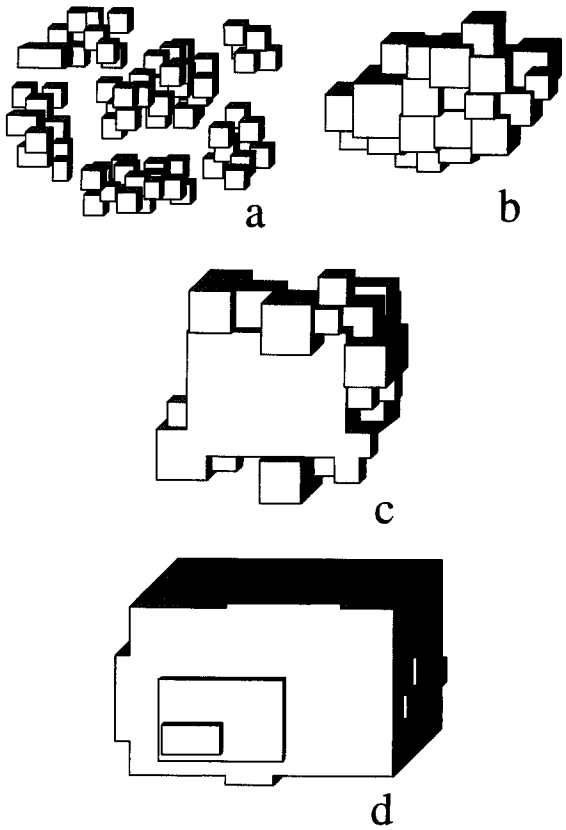

Fig. 1. Schematic drawing of the morphology of MgO samples, as obtained by HRTEM, after progressive sintering steps ((a), (b), (c), (d)).

hydroxyl groups and can be fully cleaned only by outgassing under high vacuo at $T \geq 1100$ K.

Successive exposure of such complex system to CO at room temperature, RT, gives a very complicated IR spectrum which has been the subject of many detailed investigations [55,56]. The surface species formed at RT derives from the interaction of CO with the ions located on the corners only, while the atoms on the edges and the [100] faces remain empty.

In particular the less stable and more reactive O^{2-} ions located on the corners react with CO following the path:

$$O^{2-} + CO \rightarrow CO_2^{2-}$$

$$CO_2^{2-} + CO \rightarrow C_2O_3^{2-}$$

$$C_2O_3^{2-} + CO \rightarrow C_3O_4^{2-}$$

with the formation of polymeric and conjugated species characterized by a very complicated (but nevertheless fully understood) IR spectrum (see Fig. 2, where the main attributions are also indicated).

Due to the extensive π-type conjugation some of these compounds (which testify to the high reactivity of low-coordinated O^{2-}) are highly colored [55,68]. Also the Mg^{2+} ions in corner positions react with CO at RT with formation of stable

$$Mg^{2+}_{3c} \cdots CO$$

adducts characterized by a very weak ν(CO) band at 2203 cm^{-1} (Fig. 2). This frequency, which is 57 cm^{-1} higher than that of gaseous CO, is explained in terms of polarization effects due to the high positive electric field centered at the three-fold coordinated Mg^{2+}_{3c} center [55]. When the temperature is decreased to 77 K, also the less reactive four-fold and five-fold coordinated Mg^{2+} sites located on the edges, at the steps and on the [100] facelets form CO adducts characterized by IR frequencies slightly higher than that of the CO gas (for a detailed assignment see Fig. 3a and Ref. [56]).

Also in this case the interaction of CO (through the carbon end) with Mg^{2+} is mainly electrostatic, while the oxygen ions are unreactive.

When MgO is heated in oxygen at 1100 K at increasing time, the dimension and the perfection of the microcrystals gradually increase (Fig. 1): consequently the percentage of surface atoms located on corners and on edges undergoes a dramatic decrease. This causes a parallel decrease of all the species formed on three-fold and four-fold coordinated corners and edge sites as clearly testified by the spectra reported in Figs. 2 and 3b (range, 2200–2050 cm^{-1}). To obtain a very simplified IR spectrum (Fig. 3c) indicative of a correspondingly simple surface situation, the best solid to use is the MgO 'smoke', obtained by combustion of metallic Mg (as clearly shown in Fig. 1d, which is self explanatory). The high perfection of the microcrystals is favored by the high temperature reached by the MgO particles as a consequence of the combustion reaction, a situation which allows the particles to assume the most stable crystallographic shape (lowest index faces are favored because they correspond to the minimum surface energy).

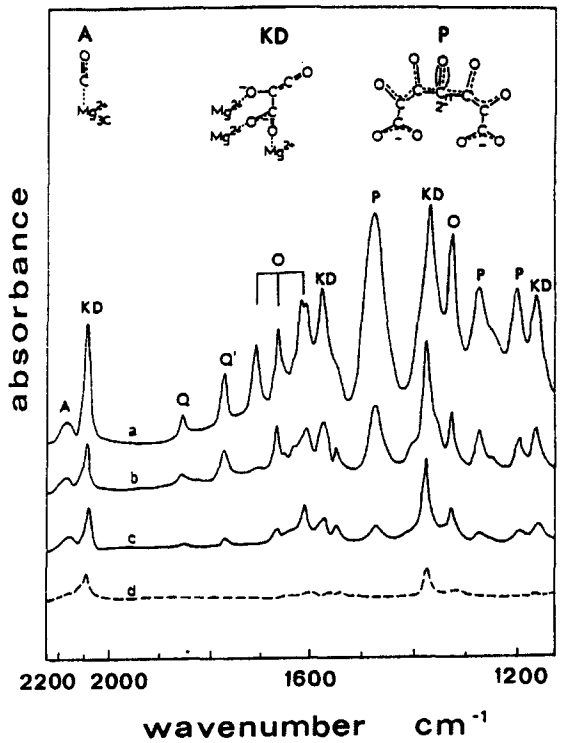

Fig. 2. Effect of the sintering temperature on the IR spectra of ^{12}CO adsorbed at 298 K (5.33 kPa) on: (a) high surface area MgO sample; (b) and (c) progressively sintered MgO samples; (d) MgO smoke. KD (trimeric) and P (polymeric) species evolve with time through fragmentation in O (oxidized, carbonate-like groups) and (Q,Q') reduced counterparts Ref. [48]. (Reproduced with permission from Elsevier.)

The only relevant ν(CO) band found on MgO smoke is observed at 2148 cm^{-1} for $\theta = 1$ and at 2157 cm^{-1} for $\theta \rightarrow 0$ (Fig. 3c). This band clearly corresponds to the stretching mode of CO polarized through the carbon end on Mg^{2+}_{5c} ions emerging on the [100] faces [57,95–97].

$$Mg^{2+}_{5c} \cdots CO$$

From Fig. 3c it can be clearly seen that not only the frequency of the peak, but also the FWHM changes with coverage, from 4.5 cm^{-1}

at $\theta = 1$, to $\cong 12$ cm^{-1} at $\theta \rightarrow 0$. Both the frequency and the half-width changes are associated with adsorbate–adsorbate interactions (mainly of the dipole–dipole type) which are gradually building up with coverage. This effect, constantly observed when an overlayer formed by aligned and perpendicular oscillators grows on a flat surface, will be more extensively treated below (vide infra).

2.2. *On the singleton frequency of CO on [100] faces and terraces of MgO: Specific and general considerations*

The frequency of CO (measured at $\theta \rightarrow 0$: singleton) adsorbed through the carbon end on Mg^{2+} emerging on the [100] faces, is shifted upward with respect to the frequency of the CO gas of $+14$ cm^{-1}. This shift is the typical result of the Stark effect associated with the positive electric field of the cation. Following Hush and Williams [98] and Pacchioni et al. [99], when no d-electrons are involved, the shift is, for moderate fields, proportional to the strength of the electric field sensed by CO adsorbed perpendicularly to the [100] face. Theoretical calculations show that the sensed field is lower than that expected for the simple complex

$$Mg^{2+} \cdots CO$$

This is not unexpected, since (on a first approximation) the effective field really sensed by CO is the result of the contribution of the part associated with the cation and of an opposite part associated with the O^{2-} anions of the first coordination sphere. When the number of anions surrounding the Mg^{2+} decreases (as on corners, edges and steps) the negative contribution to the electric field decreases and hence the 'effective' positive field sensed by CO increases. This explains very well (at least in a qualitative way) why CO adsorbed on corners is found at 2203 cm^{-1} and that adsorbed on edges and steps is found at 2165 cm^{-1}. Similar results have been obtained by Neyman and Rösch [100,101]. As the electrostatic effects can be classified as long distance effects, small inhomogeneities in the distribution of the anionic

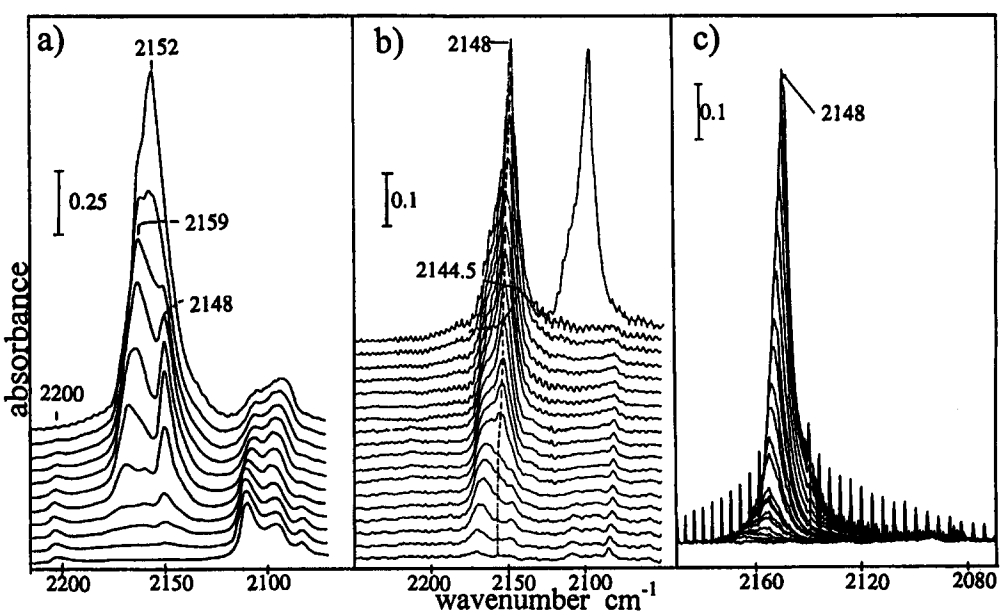

Fig. 3. IR spectra of ^{12}CO adsorbed at 77 K for coverages ranging from $\theta = 1$ (5.33 kPa) to $\theta \rightarrow 0$ on: (a) high surface area MgO sample (reproduced with permission from Elsevier); (b) sintered MgO sample; the spectrum of ^{12}CO:^{13}CO (15:85) isotopic mixture at $\theta = 1$ is also reported (reproduced with permission from the RSC, J. Chem. Soc. Faraday Trans.); (c) MgO smoke where $\theta = 1$ corresponds to 2.67 kPa (reproduced with permission from Elsevier).

and cationic sites (face borders, steps, kinks, etc.) surrounding a given singleton position on an extended face, can have small influence on the absorption frequency: this explains why, even at a very low coverage, the CO peak has a still remarkable width (for a more detailed discussion, see the next paragraph).

The considerations outlined before for MgO are of general validity and hold also for the other oxides where electrostatic forces are predominating. It will be shown in the following that when σ (like on ZnO) or $\sigma-\pi$ (like on transition metal oxides) overlap forces are contributing to the stabilization of the surface species, the singleton frequency will depend not only upon the Stark effect but also on the other contributions.

2.3. On the half width (FWHM) of the ν(CO) peak: [100] faces and terraces of MgO, specific and general considerations

For the time being let us comment only on the problem of the variation of the FWHM of the main peak on passing from high specific surface area samples (where the extension of the facelets is ca. 50 nm^2) to very low surface area smoke samples (where the extension of the faces and terraces is 10^3–10^4 nm^2). We notice that upon increasing the dimension and the perfection of the adsorbing faces, the FWHM gradually diminishes from ca. 18 cm^{-1} to ca. 4.5 cm^{-1} (data obtained for $\theta \rightarrow 1$). This observation clearly indicates that the FWHM is mainly determined by inhomogeneous broadening. In other words, the half width of the ν(CO) peak gives an indirect information about the regularity of the face where the CO molecule is adsorbed.

In order to be more quantitative, it is vital to answer the following question: what is the FWHM of the ν(CO) of an isolated CO molecule polarized through the carbon end at a Mg^{2+}_{5c} site located on infinite and perfect [100] faces? The answer is not straightforward and more information, based on data obtained on a macroscopic single crystal [100] face of MgO cut in vacuo, would be desirable. In the absence of these data, we can estimate this FWHM by considering the analogous CO–NaCl (single crystal [100] faces) system [34,35] where CO is known to be polarized on Na^{+}_{5c} ions and to have consequently a very similar frequency (ν(CO) = 2155–4 cm^{-1}). The data reported in Ref. [34] indicate a FWHM of ca. 0.25 cm^{-1} at 30 K, which is a figure definitely lower than that observed on MgO smoke (even if the higher T of the experiment on smoke suggests some caution in the comparison). From this comparison it is consequently concluded that, although the microcrystals of the smoke are appearing in the electron micrographs to expose regular [100] faces only, they must be still quite inhomogeneous at the atomic scale level, because of the presence of steps one or two atomic layers thick and of kinks. The reason for this observation can probably be sought in the preparation procedure: in fact as the MgO smoke is prepared by burning the Mg ribbon in air (which contains H_2O vapor) the surface is heavily covered by a layer of $Mg(OH)_2$, which leaves a stepped surface, upon decomposition in vacuo.

Having established that the 'natural' FHWM of the $\bar{\nu}$(CO) of CO polarized on Mg^{2+} ions located on an infinite and defect free face is lower than 1 cm^{-1}, we could speculate about the factors determining this figure; but this is largely outside the limited scope of this review. For the time being let us simply recall that the half-width could be (interalia) inversely related to the life time of the excited state and consequently to the time of decay of the vibrational excitation. Weakly bonded (polarized) CO can release the excess (vibrational) energy to the solid only with difficulty, since the bond with the surface sites is very weak: hence the life time of the excited state is high and the FWHM of the CO peak is consequently exceptionally small (as observed for the NaCl–CO system). These brief and approximate considerations are sufficient to introduce the concept that CO bonded to the surface via chemical bonds (as on

some transition metal oxides, on ZnO and on metals) should be characterized by a larger 'natural' half-width. For instance, as far as it concerns CO on metal single crystals, high resolution IR experiments have shown that the natural half width is 4–6 cm^{-1} [6,7]. We shall return to this problem in the following section.

From all the above considerations, we can conclude that the initial hypothesis, that a careful comparison of the IR spectra of CO adsorbed on progressively sintered specimens should allow a complete assignment of all the bands present on high surface area samples, is substantially correct. Similarly it is demonstrated that the spectra of CO adsorbed on (specially prepared) low surface area samples represent a good approximation to the spectra expected on single crystal surfaces.

2.4. Adsorbate–adsorbate interactions on MgO [100] faces: the shift and the intensity of the ν(CO) peak with coverage

As briefly mentioned in the previous paragraph, the main peak is observed to gradually move from 2148 cm^{-1} at $\theta = 1$ to 2157 cm^{-1} at $\theta = 0$ and this behavior has been ascribed to changes in lateral interactions. As discussed by many authors [23,102–108], in overlayers formed by very weakly adsorbed diatomic species, the interaction among the oscillators is essentially of the 'through space' type. These interactions occur among the static and dynamic dipoles of the diatomic species. Hammaker et al. [102] have calculated the effect of the dynamic dipole–dipole interactions on the CO stretching frequency as:

$$(\bar{\nu}/\bar{\nu}_0)^2 = 1 + \alpha_v T_0 = 1 + \mu_{01}^2 T_0$$

or

$$\Delta\bar{\nu} \cong 1/2\,\nu_0 \alpha_v T_0 \qquad (1)$$

where $\bar{\nu}$ is the stretching frequency at $\theta = 1$ (in the absence of static effects), $\bar{\nu}_0$ is the singleton frequency, α_v is the dynamic polarizability α $(\delta\mu/\delta Q)^2 = \mu_{01}^2$ and T_0 is the direct dipolar sum. The dynamic polarizability is proportional to the absorption coefficient and hence to the intensity of the band. Mahan and Lucas [103] have modified the previous expression by introducing the dielectric screening in the adsorbed monolayer. The modified equation is:

$$(\bar{\nu}/\bar{\nu}_0)^2 = 1 + \alpha_v T_0 (1 + \alpha_e T_0)^{-1}$$

or

$$\Delta\bar{\nu} \cong 1/2\,\bar{\nu}_0 \alpha_v T_0 (1 + \alpha_e T_0)^{-1} \qquad (2)$$

where α_e is the electronic polarizability. Similar equations hold for the static dipole–dipole shifts, whereby the $\alpha_v = \mu_{01}^2$ term is substituted by $(\mu_{11} - \mu_{00})\mu_{00}$. This also means that the through space effects have a dependence upon coverage identical to that of dynamic effects. When the interaction energies become distinctly larger than those characteristic of simple physisorption processes, other static effects must be considered as well, which more appropriately are classified as 'chemical'. These effects, being transmitted through the solid, are also named 'through solid effects'. Two types of chemical effects can be hypothesized: induction and relaxation. The first effect is associated with electronic density changes at a given site induced by adsorption at another site. This effect is absent when overlap forces are not operating (as is the case of CO on MgO: [100], where electrostatic polarization forces are absolutely predominant). The relaxation effect is a 'through solid' effect associated with changes in surface relaxation associated with adlayers formation. To explain this concept let us briefly consider the surface structure before and after adsorption. Before adsorption all the positive and negative ions are inward and outward relaxed, respectively [109,110]. Upon adsorption at a given cationic position, the positive ions move towards a more normal position and the negative ions do the same in the nearest neighbor positions and so on. Although the effect is dying away within a few spacings, it is evident that adsorption at a given site modifies the structural situation in a

small but not negligible circular area surrounding the adsorption center, so perturbing the adsorptive properties of the other cationic sites located inside. This effect is always present and is expected to have greater relevance on ZnO (because of the tetrahedral character of zinc and oxygen positions) and on high index faces of other oxides exposing ions in a lower five-fold coordination.

The value of $\bar{\nu}$ at $\theta = 1$ in the absence of dynamic effects can be evaluated with the method of the ^{12}CO–^{13}CO isotopic mixtures, suggested by Hammaker, as it corresponds to the frequency of the ^{12}CO diluted in ^{13}CO. The difference between the stretching frequency of a pure ^{12}CO-phase (where both dynamic and static contributions are present) and the frequency of the ^{12}CO peak in a diluted mixture (where only the static contributions are operating) gives $\Delta\bar{\nu}_{dyn} = 3.5$ cm^{-1} and $\Delta\bar{\nu}_{st} = -11.3$ cm^{-1}. From this, an $\alpha_v = 0.031$ Å^3 value is obtained which is not very different from that usually accepted of the free CO ($\alpha_v = 0.057$ Å^3), as expected in view of the weakness of the perturbation [111] [1].

In relation to this, it is useful at this stage to spend some effort in illustrating a few schematic (but nevertheless sufficiently general) considerations concerning the physical informations deducible from the dynamic and static shifts: these concepts are valid not only for MgO but also for the other oxides. It is well known that the value of α_v (which is the parameter directly determining the intensity of the peak) reflects the charge oscillations from the surface to the admolecule and vice-versa occurring during the CO stretching: so it depends very much upon the type of bond formed between the CO and the surface. In particular Hush and Williams [98], on the basis of the finite-field CNDO-II method, have concluded that the specific intensity decreases with the increase of the electric field. On the basis of their results the specific intensity of CO oscillators absorbing at 2203 cm^{-1} (corners) should be ca. 50% of that of CO located on [100] faces. Neyman and Rösch [100,101] have confirmed that purely electrostatic interactions decrease the intensity of the $\bar{\nu}$(CO) peak. However, when the presence of O^{2-} ions is explicitly considered on Mg_nO_n–CO clusters, embedded in an electroneutral matrix of point charges (LGCTO–LDF cluster method), an enhancement of the intensity with respect to CO gas is obtained.

Our experimental results on MgO seem to indicate an intermediate situation. We shall see in the next paragraphs that this is true also for many other oxides, where d-electrons are playing no role. Similarly a small value of α_v can be foreseen for purely σ-complexes.

On the contrary, when d–π contributions are present, the stretching of the CO (which lowers the $2\pi^*$ level) causes negative charge to flow from the adsorbing center to the CO. The opposite occurs when the CO bond is compressed. This explains the high intensity of the CO bands in metal carbonyls [98,113–119] where donation and backdonation play an outstanding role. Of course this effect is totally absent in CO adducts where only polarization forces are involved and hence no electron transfer is occurring [95–97,120]. From these brief considerations, it is evident that the evaluation of this quantity can be of great utility for elucidating the nature of the adsorbate–adsorbent interaction. Also the evaluation of the static shift is of some interest since it gives information about the permanent moments of adsorbed CO and hence on the polarization of the molecule both in the ground and in the excited vibrational state induced by the adsorption process. It is worth remarking at this point that the static shift is entirely due to dipole–dipole interactions only if 'through-solid' interactions, associated with inductive effects and surface relaxation induced

[1] Recent integrated intensity measurements [112] on the CO gas stretching mode give an integrated cross section $\sigma_s \cong 0.1 \times 10^{-17}$ cm mol^{-1} in contrast with the usually accepted value ($\sigma_s \cong 1 \times 10^{-17}$: i.e., one order of a magnitude larger). This leads to an α_v for CO gas, which is definitely lower than that usually reported in literature.

by the adsorption at a given site, play a negligible role. This is certainly true for very weak (van der Waals type) adsorption not accompanied by frontier orbital overlap and subsequent electron transfer (as on MgO). For other oxidic systems like ZnO, α-Cr_2O_3 (vide infra) this assumption is questionable.

2.5. The spectroscopy of the NiO / CO system

NiO is a cubic oxide characterized by ionicity and lattice parameters very similar to those of MgO. It is for these reasons that it forms with MgO homogeneous solid solutions with molar fraction comprised in the whole 0–1 range. Also the preparation procedure can be very similar as :(i) stoichiometric high surface area NiO is prepared (like MgO) from the hydroxide by decomposition under vacuo and (ii) low surface area materials are obtained by successive sintering at high temperature.

The evolution of microcrystal morphology on passing from high to low surface area (sintered) NiO is also very similar, as demonstrated in Refs. [60,63]: the final habit of the microcrystals is represented by nearly perfect cubelets defined by atomically flat [100] faces and terraces.

The spectroscopy of CO adsorbed on NiO samples with decreasing surface area and corresponding increase of surface perfection is represented in Fig. 4, where only the 2200–2000 cm^{-1} interval is illustrated for the sake of simplicity.

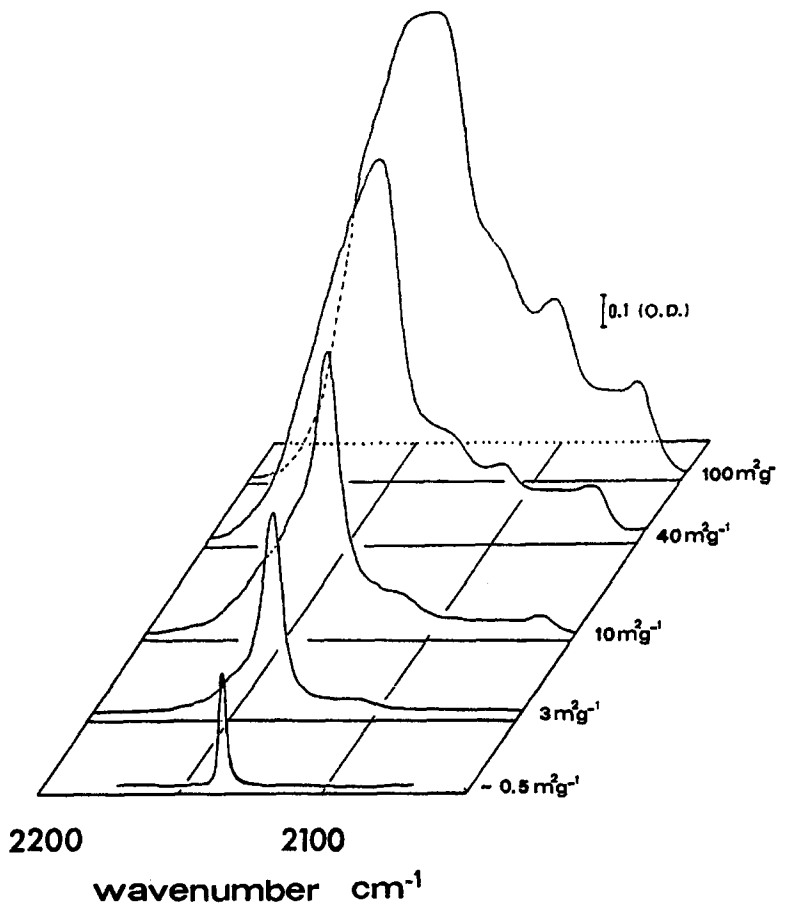

Fig. 4. IR spectra of ^{12}CO adsorbed at 77 K on NiO samples at decreasing surface area (reproduced with permission from Elsevier).

We notice the progressive simplification of the spectrum and a continuous decrease of the FWHM up to the final point where only one narrow band at 2136 cm^{-1} with FWHM = 3.7 cm^{-1} is present [63]. For the reasons already discussed for MgO, this peak must be assigned to CO adsorbed in an end-on form on five-fold coordinated Ni^{2+} ions

$$Ni^{2+}_{5c} \cdots CO$$

emerging on [100] faces and terraces. The narrow character of this band shows that the involved faces and terraces are extended and without remarkable presence of defects. The adsorption in the 2100–2050 cm^{-1} range, present only on high surface area samples, is associated with reduced nickel species, either generated during the activation procedure or formed following the path:

$$O^{2-} + CO \rightarrow (CO_2)^{2-}$$

$$(CO_2)^{2-} + 2Ni^{2+} + 3CO$$

$$\rightarrow Ni^{2+} \cdots [O_2C\text{–}Ni(CO)_3]^{2-}$$

with the formation of a species which can be interpreted as $Ni(CO)_4$ adsorbed on a $Ni^{2+}O^{2-}$ pair. The first step of this reaction, which initiates on the oxygen ions with lowest coordination number located on corners and (probably) edges, is analogous to the first step observed on MgO; only the final products are different in the two cases owing to the presence of the reducible transition metal ion [58]. By analogy with MgO the high frequency shoulders at $\bar{\nu} > 2150$ cm^{-1} correspond to CO adsorbed on 4-fold coordinated Ni^{2+} located on edges and steps and to CO on 3-fold coordinated ions in corner position. We can see here, once again, the utility of the method of progressive sintering in assigning the individual components appearing in the complex spectra of CO adsorbed on a high surface area material. Let us remark that a complex morphology of the sample is not the only source of spectroscopic complexity. In fact also non stoichiometry can play a role. In fact in the case of NiO, hydrocarbon traces can lead to

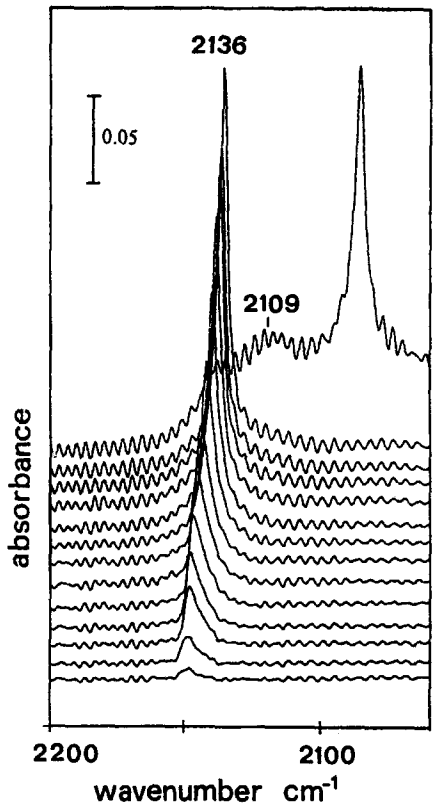

Fig. 5. FTIR spectra of ^{12}CO adsorbed at 77 K on highly sintered NiO sample for coverages ranging from $\theta = 1$ (5.33 kPa) to $\theta \rightarrow 0$ and of ^{12}CO:^{13}CO (15:85) isotopic mixture at $\theta = 1$. (Reproduced by courtesy of E. Escalona Platero et al.)

sample reduction, during the outgassing procedure, with subsequent appearance of reduced species.

Coming back to the single narrow peak observed on highly sintered NiO, we notice (Fig. 5) that it belongs to the reversible

$$Ni^{2+} \cdots CO$$

species and that its frequency gradually changes with the coverage.

We know now that this shift is associated with the changes of the adsorbate–adsorbate (static and dynamic) interactions occurring when the coverage changes from 0 to 1. With the aid of the isotopic substitution method already mentioned before, we have readily calculated that $\Delta\bar{\nu}_{dyn} = +27$ cm^{-1} and $\Delta\bar{\nu}_{st} = -43$ cm^{-1} and that $\alpha_v = 0.256$ $Å^3$ [63]. All these values are definitely higher than those found on MgO: this means that both the permanent and the dynamic

dipoles (and the associated charge oscillations from the adsorbate to the surface and vice-versa during the stretching vibration, which have direct influence on α_v [111] are substantially increased upon adsorption on NiO. This in turn indicates that the $Ni^{2+} \cdots CO$ bond has not a purely electrostatic character (as the $Mg^{2+} \cdots CO$) and that some d–π overlap forces play a small but definite role [66]. The quantification of this chemical contribution is difficult to make on the basis of our results: however by considering the modest enhancement of α_v and the very reversible character of the CO species even at low T, we conclude that chemical forces still play only a minor role. Under these circumstances the assumption that the static shift is mainly due to dipole–dipole (through space) effects can be still considered to be a valid approximation. The presence of a small backdonation explains also why the frequency of the CO peak is lower than that observed on MgO. The interaction of CO with Ni^{2+} ions has been studied by means of ab-initio methods by Pacchioni et al. [99] and by Neyman and Rösch [100,101]: in both cases the predominant role of electrostatic forces is recognized, although opposite conclusions are reached about the presence of a minor contribution of d–π overlap forces.

The discussion about the possible presence of a small contribution of d–π overlap forces at the surface of NiO is not completely academic because it can be of great help in understanding the behavior of NiO towards other adsorbates like NO (vide infra) and O_2. In fact it has been reported that the IR spectrum of O_2, adsorbed at 77 K on progressively sintered NiO samples, follows a trend similar to that observed for CO and illustrated in Fig. 4 [62]. In particular on high surface area samples, O_2^- species formed on edges, steps and corner sites are predominant, while, on progressively more sintered samples 'neutral' species adsorbed in side-on configuration on Ni^{2+} of the [100] faces, become the only observable feature of the IR spectrum.

2.6. The spectroscopy of MgO–NiO / CO system

Pacchioni et al. [99] have advanced the hypothesis that the lower stretching frequency observed for CO adsorbed on NiO (in comparison with MgO) could be simply associated with the lower ionicity of NiO which, by decreasing the positive charge localized on Ni^{2+}, has the effect of decreasing the strength of the electrostatic field centered on Ni^{2+} ions and ultimately of inducing a smaller upward shift of the CO stretching frequency. Although this hypothesis leaves the observed frequency (lower than that of the CO gas) and the observed increments of dynamic and static shifts (together with the anomalous value of α_v) unexplained, we have decided to design an experiment capable, in principle, to allow the estimation of the role of ionicity. To achieve this goal we have investigated the adsorptive properties of MgO–NiO (5% NiO) solid solutions. In our opinion these solids are properly designed for the estimation of the relative role played by d–π overlap forces and ionicity (with the related polarizing field) in determining the CO stretching frequency [66]. In fact, since the Ni^{2+} ions emerging on the [100] faces are diluted in a common MgO matrix, they should experience an environment and a ionicity extremely similar to that of Mg^{2+} emerging on the same face. On the hypothesis that chemical forces are playing no role, the frequency of CO on Mg^{2+} and on Ni^{2+} should be practically undistinguishable (because the two ions having the same radius and the same charge should also possess the same polarizing power). The experimental results shown in Fig. 6 show a different situation as the peak of CO adsorbed on Ni^{2+} ions falls at distinctly lower frequency than that of CO on Mg^{2+} (2144 cm^{-1} at $\theta \rightarrow 0$ and 2130 cm^{-1} at $\theta = 1$, $\Delta\bar{\nu}_{st} = -16$ cm^{-1}) and has an intensity larger than expected on the basis of the stoichiometry (which is an indirect indication that α_v is increased).

The -14 cm^{-1} shift observed on changing

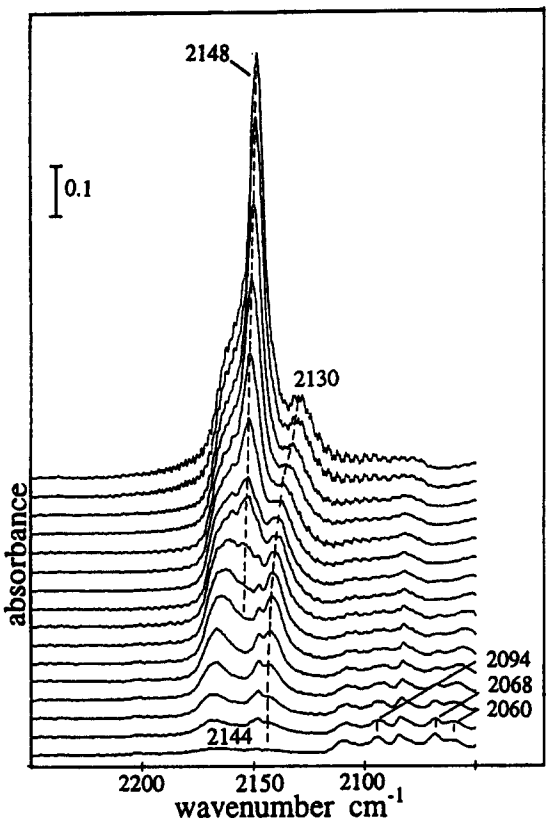

Fig. 6. FTIR spectra of ^{12}CO adsorbed at 77 K on sintered NiO/MgO solid solutions for coverages ranging from $\theta = 1$ (5.33 kPa) to $\theta \rightarrow 0$ (reproduced with permission from the RSC, J. Chem. Soc. Faraday Trans.).

the coverage, is entirely static since the CO oscillators on Mg^{2+} and Ni^{2+} are dynamically independent.

We consider these findings as a further experimental proof that in the interaction of CO with Ni^{2+} ions, the d–π contribution cannot be ignored.

2.7. The NiO / NO and the MgO–NiO / NO systems : a comparison

If the role of d–π overlap forces is quite modest in the $Ni^{2+} \cdots CO$ surface complexes, the same is not necessarily true when a stronger π-acceptor ligand like NO is used to probe the surface Ni^{2+} emerging on [100] faces of NiO or NiO–MgO solid solutions. At the same time the interaction of NO with Mg^{2+} ions emerging on the [100] faces of MgO and MgO–NiO solid solutions should still remain very weak (since only polarization forces are involved because of the absence of d-orbitals of suitable energy centered on the adsorbing Mg^{2+} center). In other words it is expected that the use of a probe molecule with greater d–π acceptor ability could add further information on the propensity of the d-orbitals to participate in the bond-formation at the transition metal centers (because it is able to amplify the d–π effects). The experimental results confirm this view, in fact: (i) on MgO and on Ni^{2+} free portions of the MgO–NiO solid solution the NO is so weakly bonded to the surface centers as to preferentially give (at 77 K) only lateral interaction products (dimerization with formation of *cis*-N_2O_2 species); (ii) on Ni^{2+} ions the situation is entirely different as $Ni^{2+} \cdots NO$ complexes stable at RT are formed. The stability of this complex together with its stretching frequency (lower than that of the NO gas) can be understood only if d-orbitals are substantially involved. The spectra regarding the NiO/NO system are illustrated in Fig. 7.

As observed for CO, the band gradually shifts with coverage because of the static and dynamic dipole–dipole interactions ($\Delta\bar{\nu}_{dyn} = 32$ cm^{-1} and $\Delta\bar{\nu}_{st} = -26$ cm^{-1}) [59]. A similar ν(NO) frequency has been observed by high resolution electron energy loss spectroscopy, HREELS. As the experimental data concerning the NO–NiO system have been reviewed in Ref. [18], the reader is referred to it for more information.

An interesting result has been obtained in an experiment where surface overlayers formed by a small fraction of NO (20%) and by a larger fraction of CO (80%) have been investigated by means of IR spectroscopy. In these overlayers, the dynamic coupling between the NO groups is negligible and consequently the position of the NO band is influenced only by the static effects associated with the surrounding CO oscillators. The NO peak in the presence of CO is downward shifted of ca. -84 cm^{-1} with respect to the value observed in absence of CO [61]. This

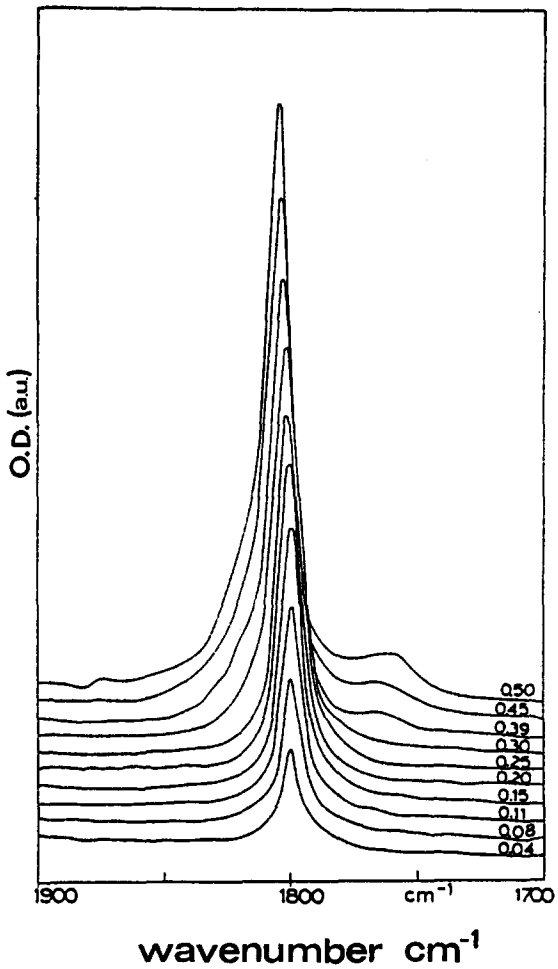

Fig. 7. IR spectra of NO adsorbed at 298 K on a sintered NiO sample for coverages ranging from $\theta = 1$ (ca. 4 kPa) to $\theta \rightarrow 0$. (Reproduced with permission from Elsevier.)

large static shift is only compatible with a model where substantial d–π contribution is present. In consideration of the increased stability of the $Ni^{2+} \cdots NO$ complexes, it is quite conceivable that the observed static shifts has not solely a 'through-space' origin.

2.8. The CoO/CO and MgO–CoO/CO systems

The results obtained with these sintered systems are entirely similar to those found with NiO and with NiO–MgO solid solutions, the main difference being represented by the smaller perfection of the CoO microcrystals even after severe sintering procedures. Because of this fact the FWHM of the CO band at 2136 cm^{-1} ($\theta = 1$) is higher than that observed on NiO; however this does not prevent a simple interpretation of the spectra [66]. The case of CoO–MgO (5% CoO) solid solutions is especially informative, as on this solid the peaks corresponding to $Mg^{2+} \cdots CO$ and $Co^{2+} \cdots CO$ adducts can be clearly distinguished (the latter being characterized by a distinctly lower stretching frequency (2118 cm^{-1}: $\Delta\bar{\nu} = 39$ cm^{-1} at $\theta \rightarrow 0$) and by a remarkable static shift with θ ($\Delta\bar{\nu}_{st} = -18$ cm^{-1}), in line with the hypothesis that d–π overlap forces are operating (Fig. 8).

Also the intensity of the ν(CO) peak of the $Co^{2+} \cdots CO$ complex is larger than expected on the basis of the pure stoichiometry: this is in agreement with the fact that the peak intensity I is proportional to α_v [111].

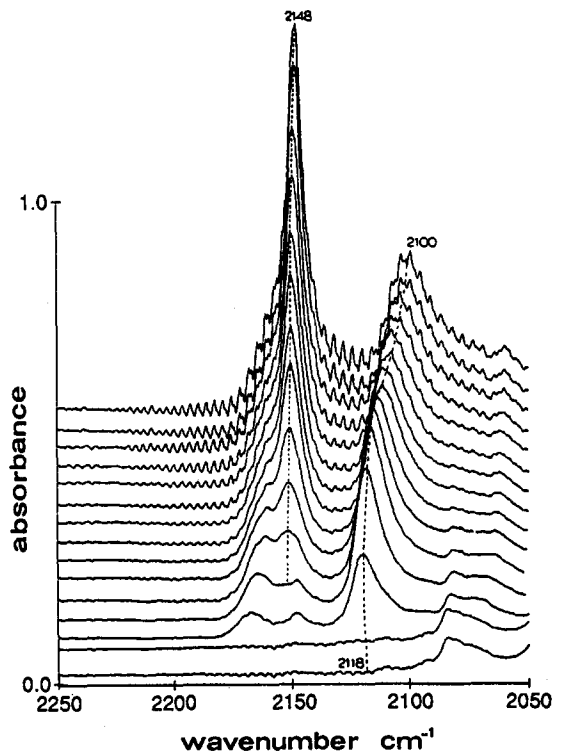

Fig. 8. FTIR spectra of ^{12}CO adsorbed at 77 K on sintered CoO/MgO solid solutions for coverages ranging from $\theta = 1$ (5.33 kPa) to $\theta \rightarrow 0$ (reproduced with permission from the RSC, J. Chem. Soc. Faraday Trans.).

The ability of d-orbitals of Co^{2+} to stabilize molecularly adsorbed diatomic species is well documented for NO [65] and particularly for O_2. In this case $Co^{3+}-O_2^-$ species in bent configuration are the main product of the interaction between O_2 and the solid solution surface [74].

3. Oxides with wurtzite structure (ZnO and diluted ZnO–CoO solid solutions)

3.1. The ZnO–CO system

When prepared by the combustion of metallic Zn, ZnO exhibits a very simple and regular hexagonal prismatic habit, where neutral $[10\bar{1}0]$ and to a smaller extent $[11\bar{2}0]$ faces dominate (Fig. 9).

On the virgin sample these faces are covered by adsorbed water and carbon dioxide: however a simple treatment under vacuo at 673 K is sufficient to completely clean them. On the contrary the same treatment is not sufficient for cleaning the non prismatic (higher index) faces, which are characterized by a higher surface energy. For this reason they remain fully covered by hydroxyl groups and do not show any activity towards the adsorption of CO probe molecules [77]. Owing to the tendency of ZnO to loose oxygen in vacuo, and hence to give non stoichiometric samples [78,79], after treatment under vacuo at 673 K, O_2 was dosed at the same temperature to restore the stoichiometry. When the surface, outgassed at 298 K and then cooled at 77 K, was exposed to increasing doses of CO, the spectra illustrated in Fig. 10 are recorded.

As discussed in detail in Ref. [77], the main peak at 2168 cm^{-1} ($\theta = 1$) (FWHM = 1.5 cm^{-1}) is associated with the CO stretching of the $Zn^{2+} \cdots CO$ complexes formed on the coordinatively unsaturated Zn^{2+} ions of the most abundant $[10\bar{1}0]$ faces (Fig. 9). For the reasons discussed in the previous paragraphs the remarkably low FHWM is a consequence of the high regularity of the $[10\bar{1}0]$ faces which keeps the inhomogeneous broadening effects to very low levels. The shoulders at 2178 and 2184 cm^{-1} are associated with $Zn^{2+} \cdots CO$ complexes of the same faces but located near the edges and the corners. The vibrational frequency of these oscillators is different as compared to that of the oscillators at the center of the faces ($\bar{\nu} = 2168$ cm^{-1}) because they are less influenced by the lateral interactions (the dipolar sum near the edges and the corners is approximately 1/2 and 1/4 of the total, in agreement with the observed frequencies at 2178 and 2184 cm^{-1}). The main peak undergoes an hyp-

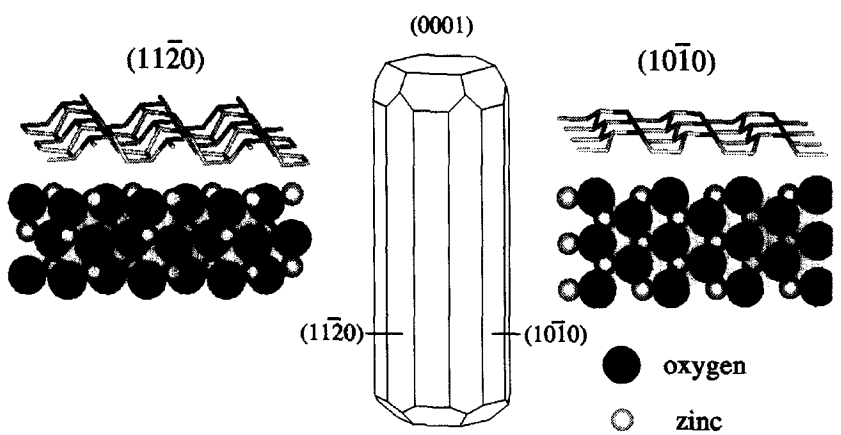

Fig. 9. Polyhedron with the indexed faces, mimicking the shape of the ZnO particles and arrangement of Zn^{2+} ad O^{2-} on $[10\bar{1}0]$ and $[11\bar{2}0]$ prismatic faces.

sochromic shift upon decreasing the coverage because of the progressive decrement of the dipole–dipole interactions (static and dynamic). By using the method of the diluted isotopic mixtures it has been determined that the total shift ($-22\ cm^{-1}$) is the sum of:

$\Delta\bar{\nu}_{dyn} = +6\,cm^{-1}$ and $\Delta\bar{\nu}_{st} = -28\,cm^{-1}$

If comparison is made with the shifts observed on NiO, we notice that the dynamic part is much lower on ZnO (about 1/4–1/5), while the static part is only approximately 1/2. As we have previously concluded that the magnitude of the dynamic shift is directly depending upon the participation of d–π orbitals to the surface–adsorbate bond, this observation is not unexpected. An important and unique characteristic of the CO–ZnO spectra is that the shift of the main band is accompanied by the appearance and disappearance of at least five narrow and discrete components, whose intensity changes as reported in Fig. 11.

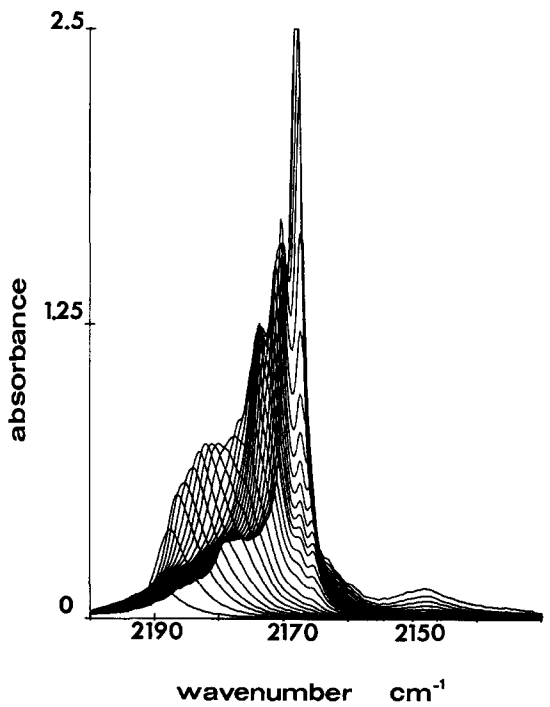

Fig. 10. FTIR spectra of ^{12}CO adsorbed at 77 K on ZnO (kadox) for coverages ranging from $\theta = 1$ (5.33 kPa) to $\theta \rightarrow 0$. (Reproduced with permission from Elsevier.)

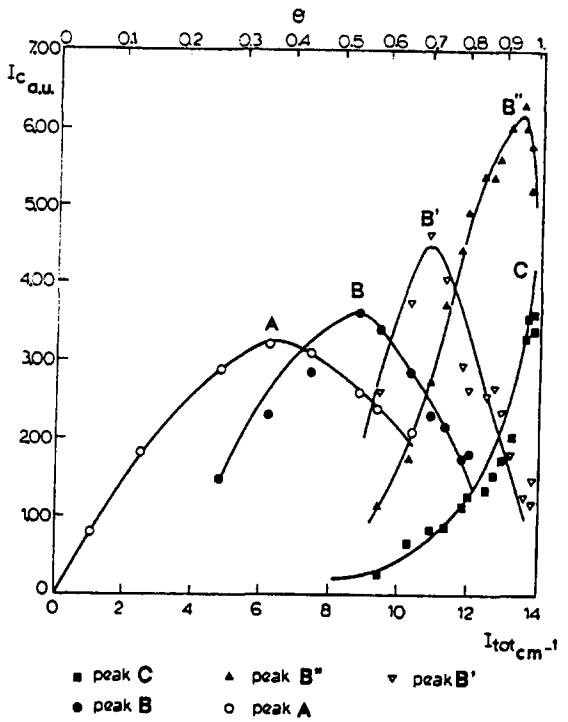

Fig. 11. Existence domain of each component as obtained by the deconvolution analysis of the spectra reported in Fig. 10: peak A in the 2190–2182 cm^{-1} range; peak B in the 2182–2177.5 cm^{-1} range; peak B′ in the 2177.5–2173.5 cm^{-1} range; peak B″ in the 2173.5–2171 cm^{-1} range; peak C in the 2171–2168 cm^{-1} range. (Reproduced with permission from Elsevier.)

These features arise from the stepwise emptying of the surface Zn^{2+} sites and correspond to differents variants of the surrounding of any given CO molecule. The five bands have been explained [77] in terms of the local arrangements, as shown in Scheme 1 where species A dominates at $\theta = 0$ and species C is the only one present at $\theta = 1$, while species B, B′, B″ are more dominant at intermediate coverages (ca. 0.5, ca. 0.7 and ca. 0.9, respectively). For $\theta \rightarrow 0$ the frequency of adsorbed CO (singleton frequency) is observed at 2190 cm^{-1}, i.e., +47 cm^{-1} shifted with respect to the CO gas. This large upward shift (when compared with that observed for the only other divalent cation Mg^{2+} without d-electrons studied so far) can be explained in terms of the greater polarizing field of three-fold coordinated Zn^{2+} ions present on $[10\bar{1}0]$ faces and in terms of the simultaneous

presence of σ-type orbital overlap contribution between the 5σ-orbital of CO and the empty dangling sp^3 hybrid with acceptor-character centered on the Zn^{2+}. Direct support for this hypothesis arises from the higher adsorption enthalpy (near 50 kJ mol^{-1}), as compared to MgO (where it is only about 15–20 kJ mol^{-1}) and from UPS results [121–123]. It is also important to remember that it has been ascertained [124] that the adsorption of CO is accompanied by surface relaxation. It is evident that due to the simultaneous presence of σ-type orbital overlap and surface relaxation effects, the static shift cannot be accounted for by static dipole–dipole interactions only.

It is at this point interesting to remark that while the singleton shift is much higher than that found on MgO, the same is not true for the dynamic shift (6 cm^{-1} instead of 3.5 cm^{-1}): this seems to indicate that polarization and σ-donation changes have modest influence on α_v (which is another way of concluding that this parameter is more sensitive to the presence of $d-\pi$ forces).

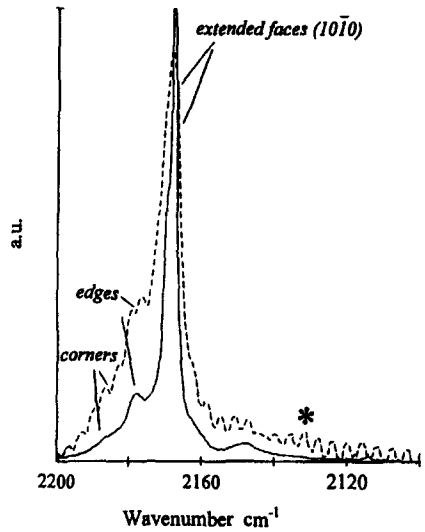

Fig. 12. Comparison between FTIR spectra at $\theta = 1$ of ^{12}CO adsorbed at 77 K on ZnO kadox and ZnO-ex-carbonate: the different specific intensities for the absorption peaks, corresponding to CO at the center of the extended face and on the edges and corners are pointed out. Star labels the rotovibrational components of the gas phase CO molecule (reproduced with permission from the RSC, J. Chem. Soc. Faraday Trans.).

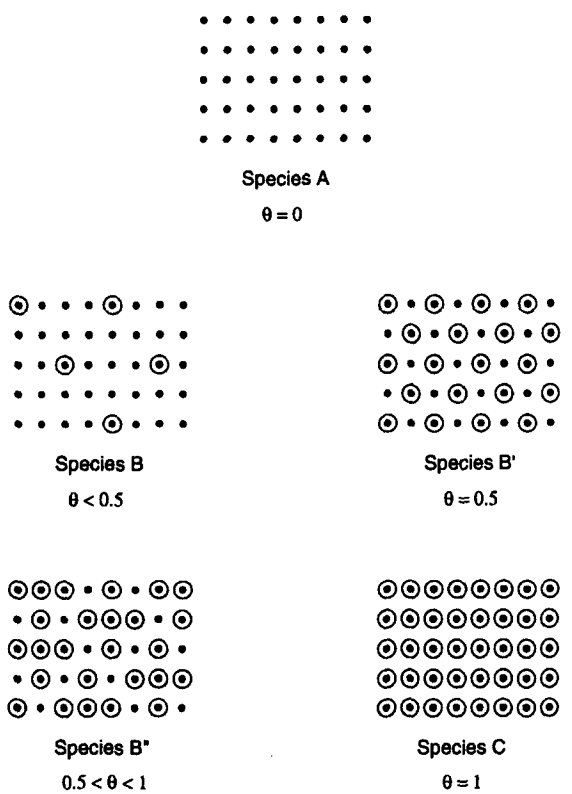

Scheme 1.

When samples with higher surface area are used (like those obtained by decomposition of $ZnCO_3$), the microcrystals have less defined morphology and the [10$\bar{1}$0] faces are less dominant and have lower areas. Correspondingly the spectrum of adsorbed CO is less intense and the band has a larger half-width (FWHM = 6 cm^{-1}).

Although the spectra obtained on the two samples are essentially similar, a careful comparison (Fig. 12) shows that the high frequency shoulders are more intense on the high surface area sample: this is in agreement with the higher amount of sites located on edges and corners.

From the previous discussion we have concluded that CO is an excellent probe of the properties of surface cationic sites because it forms $\sigma-$ type adducts with the Zn^{2+} and that oxygen sites are normally not directly involved in the interaction. However this is not always the result of the interaction with simple diatomic molecules. For instance when H_2 is

dosed on the same face, hydride and hydroxyl groups are readily formed at RT, which is indeed a clear indication that surface oxygen atoms are in this case actively participating to the adsorption process [23]. We think that what has been learnt from CO is still useful also in this case. In fact we can hypothesize that, like observed for CO, the first transient species formed upon interaction with H_2 can be a polarized form of bonded hydrogen as illustrated below:

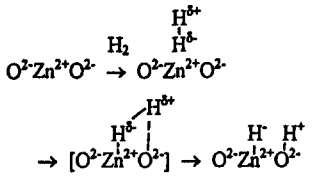

which is similar to that formed with CO. However since a greater dipole moment is induced, the polarized H_2 molecule becomes available to the nucleophilic attack by the oxygen ion in adjacent position, leading ultimately to its dissociation, with formation of hydride and hydroxyl groups. The same is happening if an hydrocarbon is dosed, since the C–H group behaves like hydrogen [125].

3.2. The ZnO–CoO / CO system

Co^{2+} is an ion with some preference towards the tetrahedral coordination [126]: for this reason diluted ZnO–CoO solid solutions, where Co^{2+} occupies the same lattice positions of Zn^{2+}, can be easily prepared from decomposition of mixed carbonates. This means that on the [10$\bar{1}$0] faces of these solids, isolated Co^{2+} emerge whose structural and ionic situation is extremely similar (if not identical) to that of the surrounding Zn^{2+} ions. This gives the unique opportunity of correctly comparing the spectroscopic manifestations of CO adsorbed on the two three-fold coordinated ions and of adding further experimental data potentially useful in the estimation of the relative role of polarization and overlap forces in determining the CO stretching frequency. The spectra obtained on this system are shown in Fig. 13. We notice that they are composed of two parts, one associated with CO on Zn^{2+} ions (2200–2150 cm^{-1}: nearly identical to that observed on pure ZnO ex-carbonate) and a second associated with CO on Co^{2+} ions (2133–2079 cm^{-1}).

It is most noticeable that the frequency difference measured at $\theta \rightarrow 0$ (singleton) between CO on Co^{2+} and CO on Zn^{2+} is remarkably large ($\Delta\bar{\nu} = -57$ cm^{-1}): this is clearly associated with the participation of d-electrons in the

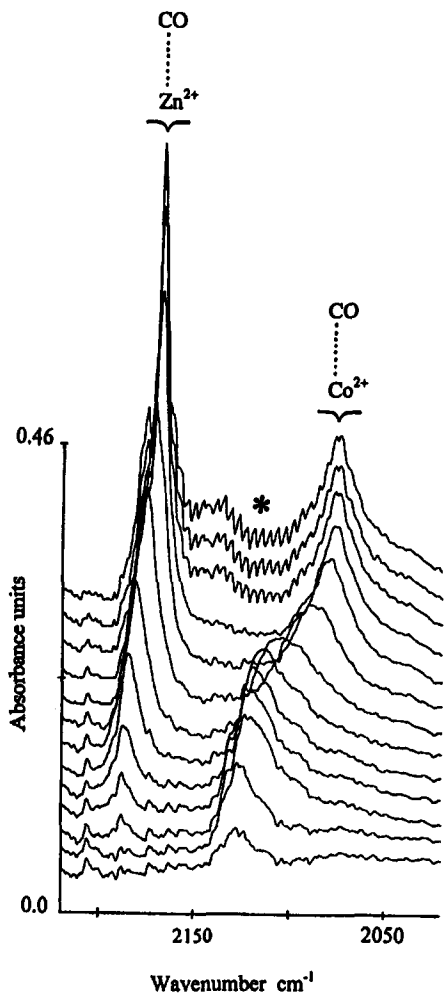

Fig. 13. FTIR spectra of ^{12}CO adsorbed at 77 K on sintered CoO/ZnO solid solution (0.05 atomic ratio) for coverages ranging from $\theta = 1$ (5.33 kPa) to $\theta \rightarrow 0$. Star labels the rotovibrational components of the gas phase CO molecule (reproduced with permission from the RSC, J. Chem. Soc. Faraday Trans.).

surface–CO bond. In connection with this observation let us remember that the interaction energy of CO with Co^{2+} is quite different from that of CO on Zn^{2+}: in fact, while the adsorption on Zn^{2+} is fully reversible at the temperature of the IR experiment, the same does not hold for CO on Co^{2+}. The larger shift (and the greater stability) observed for $Co^{2+} \cdots CO$ complexes in ZnO as compared to MgO matrix is probably associated with the different local structures of Co^{2+} sites, tricoordinated in one case (ZnO) and pentacoordinated in the second case (MgO). In the first case, due to the presence of the strong sp^3 hybrid at the adsorbing center, σ-bonding is larger and this in turn induces a stronger backdonation and subsequently a larger downward shift of the CO stretching frequency. As the surface concentration of $Zn^{2+} \cdots CO$ species increases, the band associated with $Co^{2+} \cdots CO$ progressively moves from 2133 to 2079 cm^{-1}: in view of the frequency differences of the two types of oscillators, this shift is completely static in origin ($\Delta\bar{\nu}_{st} = -54\ cm^{-1}$). When comparison is made with the analogous static shift measured on pure ZnO, we notice an increment of ca. 2.45 times: in our opinion this is a further indication that d–π overlap is playing a relevant role [127,128].

As already shown [80] additional information about the perturbation caused by the interaction with the Co^{2+} sites on the electronic structure of CO comes from the intensity of the $Co^{2+} \cdots CO$ peak (in fact the intensity is proportional to the square of the transition moment). It is a matter of fact that the intensity is 40% of the total instead of the 5% expected on the basis of the stoichiometry and of a purely electrostatic model. This increment by a 2.8 factor, is again in agreement with a substantial increase of the d–π overlap contribution on passing from $Zn^{2+} \cdots CO$ to $Co^{2+} \cdots CO$ complexes embedded in the same matrix, even if a quantification is not possible. It is evident that the result obtained with CO is totally preliminary and it is far from giving a complete picture of the properties of ZnO–CoO solid solutions. Experiments with NO, O_2 and H_2 should be performed to complete the picture.

4. Oxides with corundum structure (α-Cr_2O_3, α-Fe_2O_3, α-Al_2O_3)

4.1. The α-Cr_2O_3 / CO system

As α-Cr_2O_3 microcrystals of very regular habit can be easily prepared by combustion of

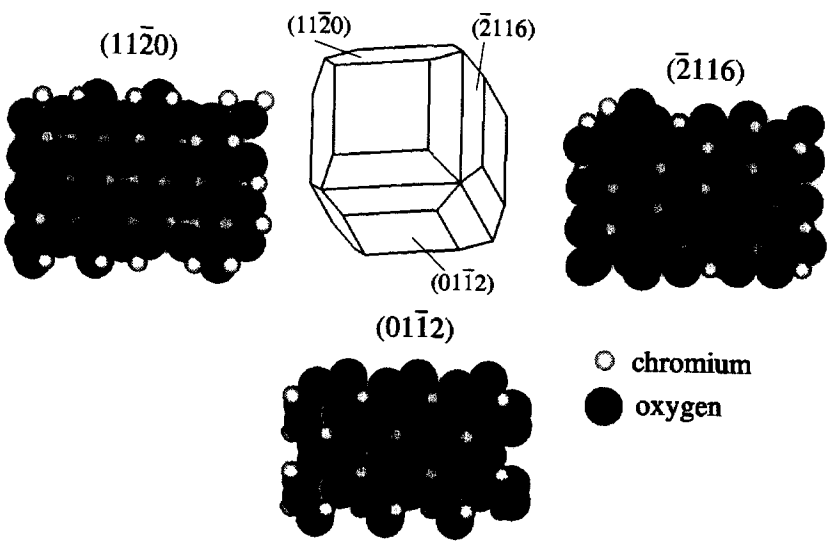

Fig. 14. Polyhedron with the indexed faces of $\alpha - Cr_2O_3$ (the extension of [01$\bar{1}$2] faces is predominant) and arrangement of Cr^{3+} and O^{2-} ions on [01$\bar{1}$2], [$\bar{2}$116] and [11$\bar{2}$0] faces.

ammonium dichromate, the spectroscopy of CO adsorbed on them has been the object of a number of detailed studies [81–86]. The morphology of the microcrystals, as determined by HRTEM and computer graphics, is represented by the polyhedra shown in Fig. 14 which expose prevalently [01$\bar{1}$2] faces and to a lesser extent [$\bar{2}$116] and [11$\bar{2}$0] faces. The ([1$\bar{1}$2] external planes are regular and essentially defect-free.

The arrangement of the Cr^{3+} and O^{2-} ions on [01$\bar{1}$2], [$\bar{2}$116] and [11$\bar{2}$0] unreconstructed faces is also shown in Fig. 14. These faces are all neutral as expected for samples which have been treated at high temperature and which consequently can assume the most thermodynamically stable morphology. This conclusion is valid for all the oxidic systems studied so far in our group and seems to possess a general validity. The [01$\bar{1}$2] faces contain an array of equivalent, 0.365 nm spaced, Cr^{3+} ions in 5-fold (square pyramidal) coordination: coordinative adsorption of CO on these sites appears most probably the result of CO adsorption with the formation of an ordered adlayer of parallel oscillators perpendicular to the surface plane. The neutral faces belonging to the [$\bar{2}$116] family contain 4-fold and 5-fold coordinated ions: these faces are certainly more reactive and could give rise to reconstruction phenomena when treated at high temperature. Due to existence of two type of ions, the spectroscopy of CO adsorbed on them should be quite complex. Finally on the prismatic [11$\bar{2}$0] faces, containing a higher density of sites, the Cr^{3+} ions are greatly shielded by the surrounding oxygen ions (which are located at an upper level). This surface hence appears quite homopolar and probably less active or even inactive towards the interaction with CO.

The typical spectra (in the 2200–2100 cm^{-1} range) of increasing doses of CO adsorbed on the same α-Cr_2O_3 sample treated at increasing temperatures under vacuo are shown in Fig. 15.

These samples are characterized by crystallites of increasing size, where the less stable faces (i.e., those containing the most coordinatively unsaturated ions) are progressively eliminated or reconstructed). This explains three ba-

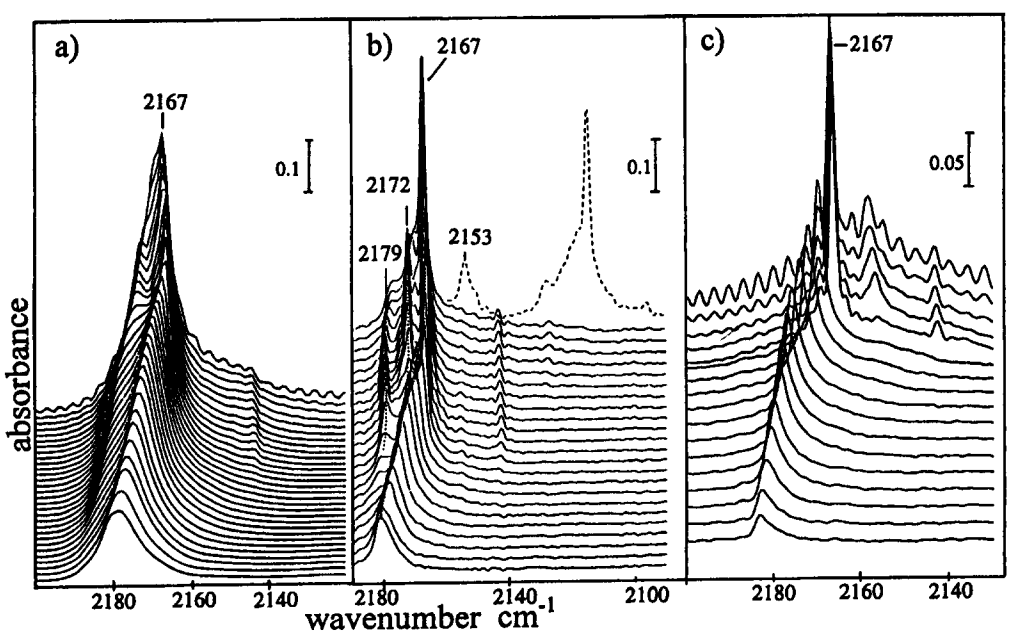

Fig. 15. FTIR spectra of ^{12}CO adsorbed at 77 K on progressively sintered α-Cr_2O_3 samples for coverages ranging from $\theta = 1$ (5.33 kPa) to $\theta \rightarrow 0$ and of ^{12}CO:^{13}CO (15:85) at a maximum coverage on (a) high surface area sample; (b) sintered sample (both reproduced with permission from Elsevier); (c) highly sintered sample (unpublished results).

sic observations: (i) the intensity of the CO stretching bands gradually decreases; (ii) the IR spectrum undergoes a progressive simplification; (iii) the FWHM of the single components gradually decreases (because inhomogeneous broadening effects associated with surface irregularities progressively lose weight). This behavior once again confirms the general applicability of the method of progressive sintering to obtain information on surface planes of high structural perfection (comparable to that obtainable, in principle, from single crystals).

For the sake of brevity we shall comment in detail only the behavior of the main peak which is the only one remaining after the most severe thermal treatments and is associated with CO adsorbed on the [01$\bar{1}$2] faces. On the contrary, only a few considerations will be devoted to CO adsorbed on the other faces (in particular on the prismatic [11$\bar{2}$0]). For more detailed information see Ref. [84,85]. The following can be briefly commented:

(i) the peak is initially observed at 2181 cm^{-1} ($\theta \cong 0$: singleton) and than gradually moves to 2167 cm^{-1} ($\theta \rightarrow \theta_{max}$). Simultaneously the FWHM decreases from 4 cm^{-1} to 1.5 cm^{-1} (data corresponding to the most sintered sample). This peak is assigned to CO adsorbed through the carbon end on Cr^{3+} ions. The remarkably small half-width observed on the last sample represents a clear indication that inhomogeneous broadening has been minimized and that the exposed [01$\bar{1}$2] faces are extended and nearly defect free;

(ii) isotopic $^{12}CO-^{13}CO$ substitution experiments (not described in detail for the sake of brevity) show that the 2181 → 2167 cm^{-1} shift is the result of two opposite effects, one dynamic ($\Delta\bar{\nu}_{dyn} = +13.5$ cm^{-1}) and one static ($\Delta\bar{\nu}_{st} = -27.5$ cm^{-1}).

When comparison of the singleton stretching frequency of CO adsorbed on five-fold coordinated Cr^{3+} and Mg^{2+} is made, we notice that the frequency of CO on trivalent ions is definitely higher. This is in line with the hypothesis that electrostatic forces are playing an important role in the formation of the surface adlayers (because the Stark effect is known to increase the stretching frequency: in fact the field holds the CO near the surface which represent a 'wall' for the vibrating molecule due to Pauli repulsion) [99]. In the case of $Cr^{3+} \cdots CO$ complexes, where the transition metal ion is in square pyramidal coordination, an empty (acceptor) d_z^2 orbital of suitable symmetry and energy is also available: consequently a σ-dative contribution may also be contributing to the induced high-wavenumber shift, even if a quantification is not possible [100,101]. Moreover we must consider also that a modest crystal-field stabilization-energy can contribute to the stabilization of the complex. If the comparison is made with the $Zn^{2+} \cdots CO$, we notice that the singleton frequency in the two cases is nearly identical: this implies that (field + σ) effects of five-fold coordinated trivalent and three-fold divalent ions are roughly equivalent. If, instead of comparing the singleton stretching frequencies, we compare the dynamic shifts and the dynamic polarizabilities, we find that the observed analogies with the previously cited case is not so stringent: in fact in the case of α-Cr_2O_3 the α_v (dynamic polarizability) is definitely higher than that expected for a surface complex where only electrostatic and σ-forces are operating. As this has been already noticed every time a transition metal ion is involved and in view of the great sensitivity of this parameter to d–π contribution, we conclude that in the $Cr^{3+} \cdots CO$ bond, beside a predominant electrostatic effect, a small proportion of σ-donation and of subsequent d–π backdonation is also present [129,130]. It is worth to recall at this stage that the adsorption of CO on these faces is also accompanied by surface relaxation [131–133].

Coming now to the [11$\bar{2}$0] faces, where the Cr centers are more heavily shielded by the O^{2-} ions in the nearest positions, we expect that the electric field generated by the positive ions is distinctly lowered and that the surface can assume a partial homopolar character. The perturbation (and the related adsorption en-

thalpy) of the CO molecule adsorbed on these sites is consequently expected to be small and the corresponding stretching frequency to be only slightly shifted upwards with respect to the gas. Of course in this case the equilibrium distance will not be small enough to allow any orbital overlap to occur (i.e., σ and d–π effects will be totally absent). It is a matter of fact that when higher equilibrium pressures are used (data not reported for the sake of simplicity) a broad feature is observed to grow at $\bar{\nu} \cong 2160$ cm^{-1}, which can be tentatively attributed to CO on prismatic faces.

The surface chemistry of well crystallized α-Cr_2O_3 can be modified by means of reductive treatments in H_2, which create oxygen vacancies (and hence Cr^{2+}) particularly on edges and corner positions [86]. It has been demonstrated that these reduced centers can easily polymerize ethene at RT [86]. The adsorption of NO on morphologically well defined samples has not yet studied in great detail. On high surface area materials [134] it is known that stable nitrosylic species are formed together with disproportionation products (N_2O and NO_2^-) and this renders the interpretation of the resulting (complex) spectra very difficult. However the higher stability of surface nitrosyls in comparison with the corresponding carbonylic species is confirmed also in this case and can be considered as a general feature of the transition metal oxide surface chemistry. The adsorption of O_2 on extended [01$\bar{1}$2], [$\bar{2}$116] and [11$\bar{2}$0] faces occurs in a dissociative way giving a variety of surface chromyl groups [2].

4.2. The α-Fe_2O_3 / CO system

This system has been studied in Ref. [135]. The microcrystals can be prepared with sufficiently defined morphology by thermal decomposition of α-FeOOH. Needle-like crystallites are formed in this way which prevalently expose prismatic faces, characterized by highly shielded Fe^{3+} ions and partial homopolar character. The situation is similar to that encountered on prismatic faces of α-Cr_2O_3. The small value of the local field together with the absence of crystal field stabilization energy (d^5) is responsible for the low stability and for the very modest high wavenumber shift of the CO stretching band with respect to the gas phase value ($\bar{\nu} = 2164$–2165.5 cm^{-1}, $\Delta\bar{\nu} = 20$–22 cm^{-1}). Also the dynamic and static shifts (calculated by means of isotopic substitution experiments and very similar to those found on MgO) [56,66], suggest that only a very modest field effect is responsible for the formation of these highly reversible surface species. In this respect it is interesting to notice that the derived α_v is definitely smaller (0.027 Å^3) than that of the CO gas (as found on MgO).

4.3. The α-Al_2O_3 / CO system

The oxide which represents the more natural counterpart of α-Cr_2O_3 and of α-Fe_2O_3 for investigating the relative role of electrostatic and chemical forces, is α-Al_2O_3, since it has an identical structure, very similar lattice parameters (the three oxides form solid solutions in all proportions) and does not possess d-electrons.

A few attempts have been made to prepare α-Al_2O_3 samples with well defined morphology by high temperature sintering of transition aluminas (γ, η). Unfortunately the low surface area samples, so obtained when studied with electron microscopy, did not reveal the simple and well defined morphology which is required for the purposes of this investigation. In fact the particles were irregularly shaped, with only limited sizes of flat facelets; consequently we were not able to establish the indices of the most frequently exposed faces. Despite these difficulties, the spectroscopic results concerning the $Al^{3+} \cdots CO$ adducts formed at low temperature, are not without interest. They can be shortly summarized as follows [87]:

[2] Unpublished results.

(i) the CO stretching frequency is constantly higher than that of gaseous CO, though the shift is very small ($\Delta\bar{\nu} = 20\ cm^{-1}$);

(ii) the half width is very large (ca. 20 cm^{-1}) as expected for a poorly morphologically defined sample where inhomogeneous broadening effects are necessarily predominating;

(iii) the surface species are highly reversible even at low T.

The observed frequency and the weak adsorption enthalpy is very similar to that of the CO species characteristic of the prismatic faces of chromia and ferric oxide: this suggests that the same type of homopolar faces are predominant on α-Al_2O_3. The reason of the predominance of these faces characterized by highly shielded cations, can be related to the high temperature of sintering needed to form the α-phase, a parameter which could favor the preferential formation of this type of rather homopolar faces. Another possible interpretation is that at the high T needed to form the α-phase, the surfaces are all relaxed with an inward movement of the cation towards a more shielded position (and subsequent decrease of the local electric field centered on the cations) [133,136,137]. In the absence of samples with greater morphological definition, it is not possible to decide on the two different hypothesis.

It is evident that further efforts will be devoted by our group to prepare better defined samples. A further and obvious direction of investigation will be also based on the preparation of well shaped microcrystals of α-Al_2O_3/α-Cr_2O_3 solid solutions.

5. Oxides with spinel-type structure

The family of oxides with spinel-type structure is very rich and, in principle, very useful for the type of study planned with the line of investigation described in this review. In fact it should allow the systematic study of the surface CO (and NO) adducts of a great number of transition and non transition metal ions embedded in a common structure. Among the members of this class of compounds we can mention: γ- and δ-Al_2O_3 (defective spinels), $MgAl_2O_4$, $MgCr_2O_4$, $ZnCr_2O_4$, $CuCr_2O_4$, $CoCr_2O_4$, etc., characterized by a variety of different ions in two different coordination states (tetrahedral and octahedral) [138–140]. Only in the case of transition aluminas are we dealing with the same element (Al^{3+}) in 4-fold and 6-fold coordination states. Despite the great number of members of this class of stable oxides, the number of investigation carried out on well crystallized systems with sufficiently defined morphology is very scarce: in the following we shall review shortly what is known in this field. As far γ- and δ-Al_2O_3 is concerned, the reader is also addressed to the specific review contained in this book.

5.1. γ- and δ-$Al_2O_3(Al^{III}_{21+1/3}\square_{2+2/3}O_{32})$/CO systems

There are many hypotheses concerning the nature and the relative abundance of the most frequently exposed faces of microcrystalline transition aluminas [88,89,139]: unfortunately the only certain conclusion emerging from these studies is that the habit of the microcrystals is very much influenced by the preparation method, which is indeed not the best starting point for the present study.

In a spectroscopic study conducted on the CO adsorption on a γ-phase obtained by decomposition of alum [88], two main IR bands at 2210–2180 and at 2165 cm^{-1} were observed at 77 K, which were attributed to CO species polarized on the two different types of sites (containing ex-tetrahedral and ex-octahedral Al^{3+} ions) emerging on the surface. The attribution was based mainly on the simple observation that the lower frequency band coincides both in frequency and reversibility with that observed on α-Al_2O_3 (where the sites are all ex-octahedral). Unfortunately the morphology of the γ-sample was not studied in detail: this was preventing a more detailed analysis of the

location of two types of sites. Recently Marchese et al. [89] have conducted a combined IR and morphological study with HRTEM on Alon C, which is a δ-phase with tetragonally distorted spinel structure exposing prevalently [110] faces. The spectra of adsorbed CO at 77 K are reported in Fig. 16.

For the scope of this review we are interested only in the main peak centered at 2184 cm^{-1} at $\theta = 1$ and at 2204 cm^{-1} at $\theta \rightarrow 0$ ($\Delta\nu = -20$ cm^{-1}). This peak is very similar to that observed on the γ-phase and attributed to CO adsorbed on sites containing ex-tetrahedral aluminum (Fig. 17).

Similarly to what was observed on the γ-phase, the FWHM of this band is 14–26 cm^{-1}: this implies a consistent inhomogeneous broadening not only associated with the small dimension of the facelets but also with the disordered character of cations arrangement associated with the presence of cationic vacancies (□). This problem, common to all transition aluminas, represents a severe limitation for the scopes of this investigation.

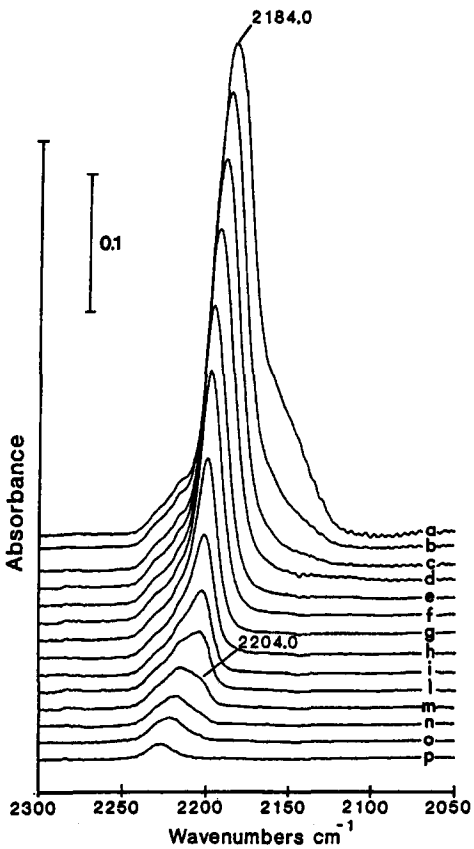

Fig. 16. FTIR spectra of ^{12}CO adsorbed at 77 K on δ-Al_2O_3 (Alon C) for coverages ranging from $\theta = 1$ (0.27 kPa) to $\theta \rightarrow 1$ (reproduced with permission from the RSC, J. Chem. Soc. Faraday Trans.).

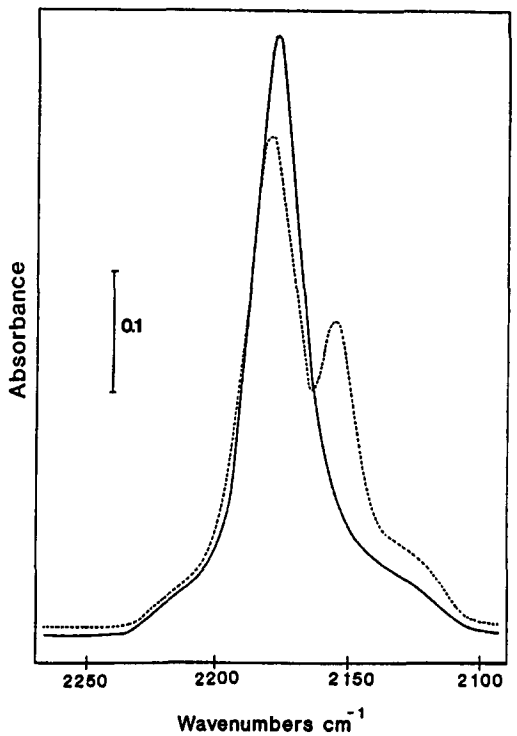

Fig. 17. Comparison between the FTIR spectra of ^{12}CO (0.07 kPa) adsorbed at 77 K on δ-Al_2O_3 (Alon C) (—) and γ-Al_2O_3 (ex-Alum.) (---) (reproduced with permission from the RSC, J. Chem. Soc. Faraday Trans.).

With respect to CO gas, the peak is shifted to higher wavenumbers by 61–41 cm^{-1}, i.e., a figure which indicates that the positive centers possess a high polarizing power. Moreover experiments with isotopic ^{12}CO–^{13}CO mixtures have shown that the dynamic part of the shift $\Delta\bar{\nu}_{dyn} = +3.6$ cm^{-1} is consistent with an $\alpha_v = 0.03$ $Å^3$. The dynamic shift and the related α_v are similar to those observed on MgO, ZnO and α-Fe_2O_3, i.e., all solids where polarization and σ-forces are dominating. As a final consideration let us recall that the adsorption of CO is clearly accompanied by surface relaxation [13,132,140].

5.2. Other spinels

To our knowledge there are no other systematic studies on the spectroscopy of CO (and NO) adsorbed on non defective spinel structures of well defined morphology: consequently this area is waiting for a systematic investigation. The main difficulty to be surmounted is the discovery of sample preparation and thermal treatment methods capable of furnishing microcrystals of well defined morphology.

6. TiO_2 (anatase and rutile)

The surface properties of TiO_2 have been the subject of many investigations devoted to correlating the Lewis acidity to the crystal structure [28–30,90,92]. CO has been often used as a probe molecule for testing the Lewis acidity mainly at RT, i.e., in conditions where only a few per cent of the surface sites can adsorb CO. Only low temperature experiments can give a realistic picture of all the surface sites exposed on the external surface.

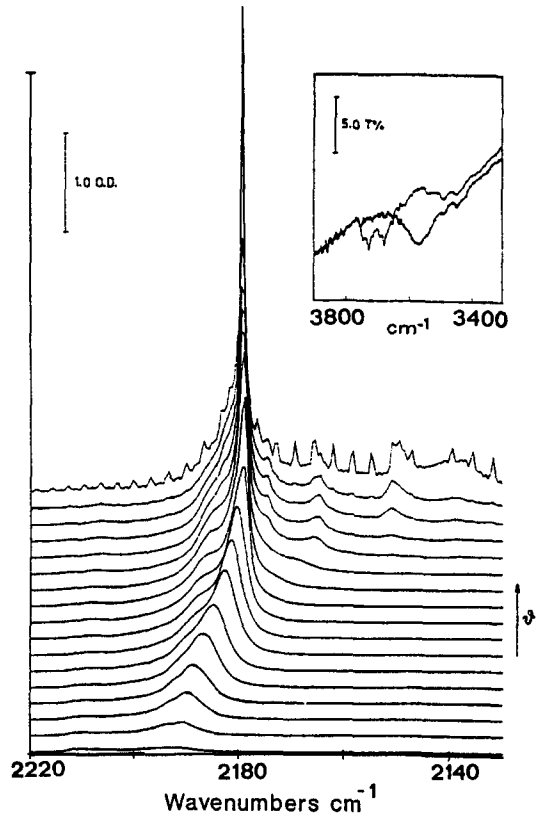

Fig. 18. FTIR spectra of ^{12}CO adsorbed at 77 K on TiO_2 sample outgassed at 873 K for coverages ranging from $\theta = 1$ (5.32 kPa) to $\theta \rightarrow 0$; in the inset: spectra in the OH region before (—) and after (· · ·) contact with CO.

6.1. The anatase / CO system

Early IR data reported by Tsyganenko et al. [141,142] concerning CO adsorbed on microcrystalline anatase at 77 K, have revealed that the spectra consisted of very narrow components, suggestive of the absence of important inhomogeneous broadening effects and hence of the presence of very regular surface planes. This result has encouraged us to further investigate this system by means of the combined use of high resolution FTIR spectroscopy and HRTEM.

The IR spectra of CO adsorbed at 77 K on Titanoxid P25 (Degussa) outgassed at 873 K are shown in Fig. 18.

The electron micrographs have shown that the microcrystals are preferentially constituted by well shaped prisms essentially exposing the [010], [101] and [001] faces, the former one being definitely more abundant than the other two [90]. It is worth noticing that on the most abundant faces the exposed Ti^{4+} are in five-fold (square pyramidal) coordination. On the basis of this conclusion about the microparticles morphology, the strong and extremely narrow peak at 2179.5 cm^{-1} (FWHM = 1.5 cm^{-1}) is assigned to CO polarized on 5-fold coordinated ions. The peak undergoes a gradual shift from 2179.5 to 2192 cm^{-1} (total shift $\Delta\bar{\nu} = 13$ cm^{-1}) upon decreasing the coverage. By using the diluted isotopic mixtures method the total shift is found to be due to the sum of a dynamic contribution $\Delta\bar{\nu}_{dyn} = +3.5$ cm^{-1} and by a static contribution $\Delta\bar{\nu}_{st} = -16.5$ cm^{-1}. These figures are typically those expected when polarization forces only are present. Also the $\alpha_v = 0.025$ $Å^3$

is in line with the hypothesis that the surface bonds are dominated by electrostatic forces.

When the anatase is sintered at higher T (1173 K), the narrow peak described before, completely disappears [92] while lower frequency (but broader) bands show up. These bands are associated with more weakly bonded surface adducts (similar to those found on α-Al_2O_3). For the time being, it has not been established if this is due to a morphological transformation or to a surface relaxation occurring on the [010] face (or to both).

6.2. The rutile / CO system

Rutile is the TiO_2-phase stable at $T \geq 1000$ K. When this sample is outgassed at $T = 1173$ K and then contacted at 77 K with CO, only very weakly adsorbed species absorbing at 2175 and 2156 cm^{-1} are observed (the second band

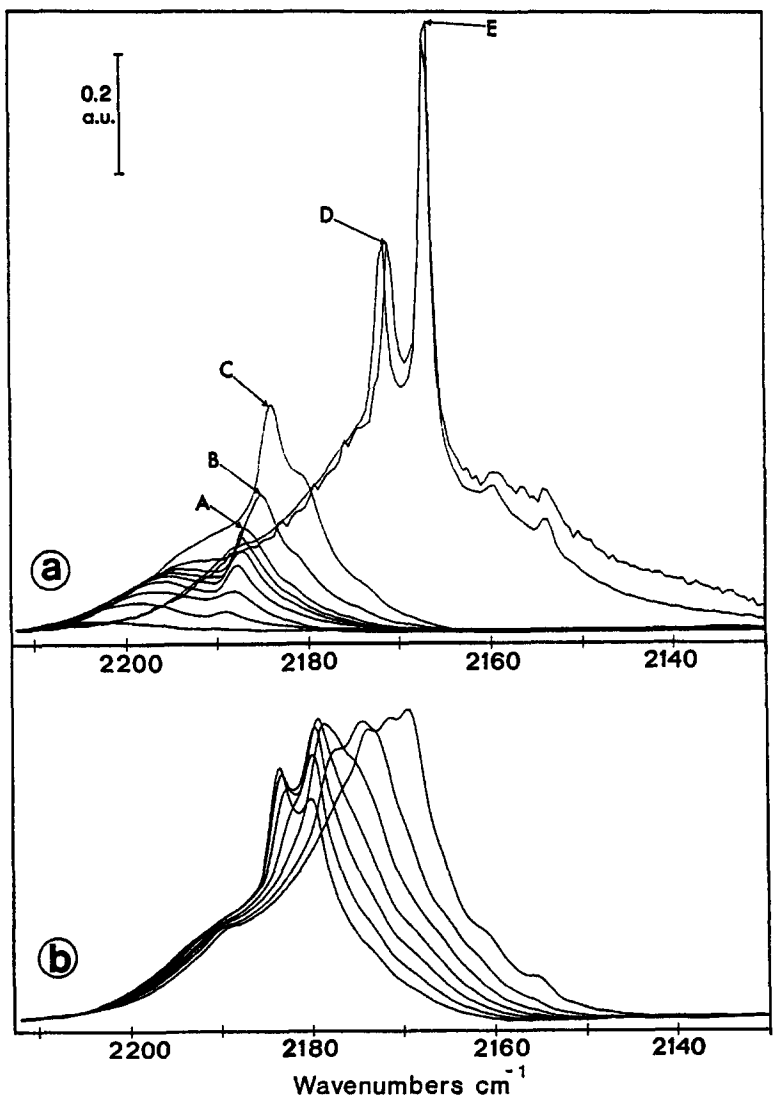

Fig. 19. FTIR spectra of ^{12}CO adsorbed at 77 K on ZrO_2 samples: (a) high and low coverages ranging from $\theta = 1$ (5.33 kPa) to $\theta \rightarrow 0$ (1.33×10^{-5} kPa); (b) intermediate CO coverages. (Reproduced with permission from Elsevier.)

being definitely more intense) [92]. On the basis of the reported information it is difficult to associate these bands with specific faces. However this information seems to confirm a general observation: when oxides are treated at very high temperature under vacuo, they all show the tendency to expose surfaces with increasing homopolar character. In our opinion this is likely due to a relaxation process occurring at high temperature which is accompanied by an inward movement of the cations, with subsequent decrease of the polarizing capacity and of the degree of insaturation.

7. The CO/ZrO_2 system

In 1991, Morterra et al. [93,94] have investigated the spectroscopy of CO adsorbed at 77 K on a highly sintered ZrO_2 specimen and the resulting spectra at increasing coverages are illustrated in Fig. 19.

As the authors have noticed, there is a great similarity between this spectral series and that presented for the ZnO/CO system, the main difference being represented by the presence at $\theta = \theta_{max}$ of two very narrow bands at 2172 and 2167 cm^{-1} (HWFM $\cong$ 3–3.5 cm^{-1}) instead of the single one observed on ZnO. This probably reflects the presence of two well developed and defect-free faces on the microcrystals. As observed on ZnO by decreasing the coverage, new bands appear and disappear giving a very complex but nevertheless interesting pattern. This complicated envelope corresponds to different CO surroundings on the two faces. The peak at 2167 cm^{-1} has been tentatively ascribed to CO adsorbed on [111] faces, where the Zr^{4+} ions are 0.35 nm apart and form a rhombohedric array. By using the method of the diluted isotopic mixtures, the dynamic and the static shifts have been evaluated: $\Delta\bar{\nu}_{dyn} = +3\ cm^{-1}$, $\Delta\bar{\nu}_{st} = -25\ cm^{-1}$. From the first figure an $\alpha_v = 0.024$ $Å^3$ can be readily calculated, which suggest that electrostatic polarization forces are mainly involved. Notice that the static shift is very near to that observed on ZnO.

8. Final considerations

8.1. Structure of CO adsorbed on extended faces

On low index faces of oxides, the CO molecule is invariably adsorbed through the carbon end on surface cations forming ordered surface adlayers of parallel oscillators. The $Me^{x+} \cdots CO$ bond (Me^{x+} = non transition metal ion or transition metal ion in a d^5 configuration) is always dominated by electrostatic field effects leading to the polarization of the molecule and to an increase of the stretching frequency which is roughly proportional to the polarizing field [129,130]. The effect of this polarization (not accompanied by charge flow from the molecule to the surface) on the static and dynamic dipole moments is very modest. In one case (Zn^{2+} in trigonal coordination) a substantial contribution of σ-bonding has been ascertained. If the α_v values obtained on non transition metal oxides are plotted against the CO stretching frequencies (Fig. 20) we notice that they are all included within a small interval.

In the same figure the α_v values of CO gas are also reported [111,112] (open and closed squares) and for the sake of completeness the α_v of CO adsorbed on alkali halides (where electrostatic forces are only involved) are reported (open triangles) [54]. Taking this all together, these data indicate that the intensity of the peaks of CO, polarized by the Stark effect, included in the 2200–2143 cm^{-1} interval are not very much influenced by the strength of the polarizing field. Essentially similar conclusions have been reached in Ref. [112] by means of combined spectroscopic and volumetric experiments.

When transition metal cations are involved, a small contribution to the bond stability comes also from d–π overlap forces which greatly influence the static and the dynamic dipoles

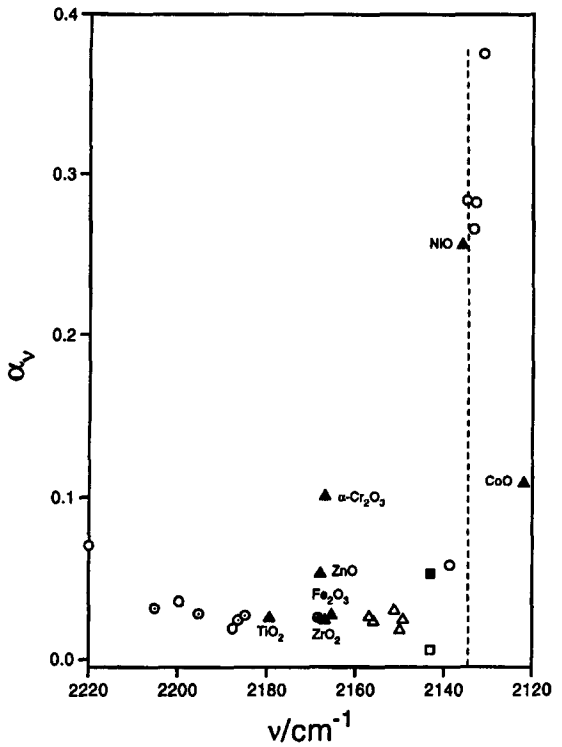

Fig. 20. Dependence of α_v upon $\bar{\nu}$: ○ data from Ref. [111], ■ CO gas, data from Ref. [111], □ CO gas, data from Ref. [112], △ present work, ⊙ data from ref. [91], ▲ data from Ref. [54], ⊕ data from Ref. [142].

localized on adsorbed CO. The dipole–dipole interaction occurring in the ordered adlayers is hence invariably greater on transition metal oxides surfaces with respect to the non transition ones (with the exception of Fe_2O_3 which behaves more as a non transition metal ion, probably because of its d^5 configuration) (closed triangle in Fig. 20). All the data concerning non transition and transition metal ions are collected in Fig. 20. The vertical broken line intersecting the abscissa at about 2135–30 cm^{-1} indicates schematically the narrow region where a small change of the CO frequency is accompanied by dramatic increase of the dynamic polarizability and hence of the intensity. The region on the right hand side is the typical one of low-valence or zero-valence metal carbonyls which are characterized by powerful d–π overlap and hence by intensities (per oscillator) and α_v values which can be two orders of magnitude larger than those of CO [98,113,114]. In the region comprised in the 2140–2200 cm^{-1} interval all values concerning non transition metal oxides or α-Fe_2O_3 (d^5) have very small values (similar to that of free CO) which are all included in a very narrow interval: this indicates that polarization and/or σ-bonding have little effect on α_v. From all these considerations it is once more emerging that the parameter most sensitive to d–π overlap forces is definitely the dynamic polarizability. The steep rise of this parameter occurring preferentially at ca. 2135 cm^{-1}, also indicates that an increment of d–π contribution having little effect on the stretching frequency can have dramatic consequences on the dynamic polarizability and on the intensity. On this basis we can understand the apparent exception represented by CO on α-Cr_2O_3. This is a case where, despite the high stretching frequency (indicative of a predominant electrostatic field effect), a very small, but nevertheless not negligible, d–π contribution is present which, although it does not appreciably decrease the stretching frequency (and the force constant), it increases the dynamic polarizability.

The half-width of the CO stretching peak is strongly influenced by inhomogeneous broadening effects: consequently it is a very sensitive parameter of the perfection of the adsorbing surface. In a few cases (ZnO, α-Cr_2O_3, NiO, TiO_2 and ZrO_2) FWHM values comprised in the 1.5–3.7 cm^{-1} interval have been obtained which are indeed remarkably low figures for polycrystalline materials. This indicates that, when suitable preparation procedures are adopted, high quality spectroscopic results can be obtained also on polycrystalline materials.

8.2. *Structure of NO on extended faces*

Although the data concerning NO are much less abundant, a few general considerations can be derived which can be summarized as follows:

(i) On non transition metal oxides NO is very weakly adsorbed (like CO). However, unlike

CO, the adsorbate–adsorbent interaction energy is weaker than the adsorbate–adsorbate interaction (because NO, being a radical has a distinct tendency to dimerize): consequently the surface species are invariably dimeric and the related spectroscopy consequently very complex.

(ii) The interaction energy of NO with transition metal cations is usually larger than that observed for CO and more stable (linear) mononitrosylic species are consequently formed. The NO–NO interaction (when studied in detail) resulted to be of a dipole–dipole type and to be associated with large frequency shifts of the NO band with the coverage. Due its higher $d-\pi$ acceptor ability, the NO probe adds further information on the propensity of the d-orbitals of surface transition metal cations to participate to the bond formation and stabilization. In other words NO behaves (with respect to CO) as an efficient amplifier of $d-\pi$ overlap effects.

8.3. Surface relaxation

In highly sintered specimens treated for a long time at very high temperature, a general tendency of the positive cations to move towards more shielded positions is often observed, with a parallel decrease of the polarization forces and a remarkable development of homopolar character. This point deserves further experimental investigation.

As far as the surface relaxation on samples treated at lower temperature is concerned, let us stress that the surface models illustrated in Figs. 9 and 14 have purely geometric character and ignore the possible presence of important relaxation effects affecting the positions of cations and anions and consequently influencing the electric fields associated with them (and the effective availability of the frontier orbitals as well). This problem is certainly of major importance for ZnO and for the surface sites located (in the bulk) in tetrahedral position (spinels). As computational programs of surface relaxation are gradually becoming available [131], there is matter of comparison on the theoretical predictions with accurate measurements of surface fields. As we have seen in the text, CO is a sensitive probe of local positive fields centered at the cationic sites (since it is known that there is a direct proportionality relation between the frequency shift from the gas phase value and the perturbing electric field): hence we see here a developing field of investigation.

8.4. CO (NO) adsorbed on low coordinated (defective) cationic sites

Although this point is not representing the specific argument of this paper, it merits few considerations.

Low coordinated cationic sites are located at the edges, steps and corner sites of microcrystals. When heavily sintered oxides are studied, the number of these sites is very low and their influence on the overall surface reactivity is consequently very modest.

On the contrary, when high surface area materials are investigated, the contribution of these sites cannot be ignored as it often determines the catalytic properties of the solid. From the experimental results illustrated in the text and from the immense literature on dispersed oxides available [129,130] a few general rules can be extracted which can be summarized as follows: (i) the polarizing field of low coordinated cations is larger than that observed for cations on low index faces; (ii) the low coordinated transition metal cations are more easily reduced by hydrogen than ions located on extended faces; (iii) low coordinated transition metal ions are in general terms more reactive as they adsorb dissociatively hydrogen and easily form O_2^- species by interaction with oxygen (Ni^{2+}, Co^{2+}); (iv) low coordinate surface cations adjacent to low coordinated oxygen ions (like on special defects of cubic oxides or on ZnO) can generate a peculiar chemistry, where the Lewis acid properties of the cation and the basic properties of the anion (vide infra) combine in a synergic way. The case of the $ZnO–H_2$ system is very illustrative of this.

8.5. The role of surface oxygen ions

When CO and NO are used as surface probes of low index faces, they form bonds only with metal cations: so the oxygen ions reveal their presence in an indirect way, simply because they act as spacers and because they decrease the electric field sensed by the probes at the cationic positions. However oxygen ions located on edges and steps or on corners can have a so low Madelung stabilization energy to become distinctly nucleophilic, so attacking also robust molecules like CO and NO molecularly adsorbed on adjacent cations, with formation of a complex variety of anionic species (MgO, NiO).

8.6. Extension to other probe molecules

From the results briefly reviewed in the paper, we have seen clearly that the surface properties probed by a molecule do not only depend upon the structure of the probed surface, but also upon the structure of the molecule itself. The case of ZnO is fully illustrative of this concept: in fact while CO is forming a bonding only with the surface cations, H_2 interacts with both cations and anions leading to the dissociation of the molecule. From this, it is evident that the surface properties of morphologically well defined microcrystalline oxides must be probed with a larger variety of molecules. We think that the most obvious extension of our work should be in the direction of H_2 and O_2 also because they are involved in many catalytic reactions.

8.7. Conclusions

As a very final consideration, it must be admitted that the results illustrated in this review are still highly incomplete and that this area is still in a very primitive stage of development. It is evident that new data on other oxides like spinels and perovskites (necessary to complete the picture) would be welcome together with more accurate data concerning the already described oxides. The whole subject will of course benefit of the simultaneous appearance of data obtained on macroscopic single crystals or on well defined films.

Acknowledgements

This research was supported by CNR, Progetto Strategico Tecnologie Chimiche Innovative and MURST.

References

[1] H. Pfnür, D. Menzel, F.M. Hoffmann, A. Ortega and A.M. Bradshaw, Surface Sci, 93 (1980) 431.
[2] R.F. Willis, A.A. Lucas and G.D. Mahan, in D.A. King and D.P. Woodruff (Editors), The Chemical Physics of Solid Surface and Heterogeneus Catalysis: Adsorption at Solid Surface, Elsevier, Amsterdam, 1983, p. 59.
[3] S. Haq, J.G. Love and D.A. King, Surface Sci., 275 (1992) 170.
[4] L.D. Mapledoram, A. Wander, D.A. King, Surface Sci., 312 (1994) 54.
[5] A.M. Bradshaw, Appl. Surface Sci., 11/12 (1982) 712.
[6] M.A. Chesters, S.F. Parker and R. Raval, Surface Sci., 165 (1986) 179.
[7] R. Raval, S.F. Parker, M.E. Pemble, P. Hollins, J. Pritchard and M.A. Chesters, Surface Sci., 203 (1988) 353.
[8] A. Crossley and D.A. King, Surface Sci., 95 (1980) 131.
[9] E. Borguet and H.L. Dai, J. Chem. Phys., 101(10) (1994) 9080.
[10] N. Sheppard and T.T. Nguyen, in Advances in Infrared and Raman Spectroscopy, Vol. 5, Heyden, London, 1978, Chap. 2.
[11] A.P. Hagan, M.G. Lofthouse, F.S. Stone and M.A. Trevethan in Louvain la Neuve (Editor), Scientific Bases for the Preparation of Heterogeneus Catalysts, 1978, p. 1.
[12] A. Zecchina, S. Coluccia and C. Morterra, Appl. Spectrosc. Rev., 21(3) (1985) 259.
[13] A. Zecchina and D. Scarano, in Adsorption and Catalysis on Oxide Surfaces, Elsevier, Amsterdam, 1985, p. 71.
[14] A. Zecchina, G. Spoto and D. Scarano, J. Electron Spectrosc. Rel. Phenom., 45 (1987) 269.
[15] S. Coluccia, in C. Morterra, A. Zecchina and C. Costa (Editors), Structure and Reactivity of Surfaces, Elsevier, Amsterdam, 1989, p. 289.
[16] G. Ghiotti, F. Boccuzzi and A. Chiorino, Mater. Chem. Phys., 29 (1991) 65.
[17] A. Zecchina and C. Otero Areán, Catal. Rev. Sci. Eng., 35(2) (1993) 261.
[18] J. Sauer, P. Ugliengo, E. Garrone and V.R. Saunders, Chem. Rev., 94 (1994) 2095.

[19] A.A. Tsyganenko and V.N. Filimonov, J. Mol. Struct., 19 (1973) 579.
[20] I.E. Wachs, F.D. Hardcastle and S.S. Chan, Spectroscopy, 1(8) (1986) 30.
[21] M.A. Vuurman and I.E. Wachs, J. Phys. Chem., 96 (1992) 5008.
[22] N. Das, H. Eckert, H. Hu, I.E. Wachs, J.F. Walzer and F.J. Feher, J. Phys. Chem., 97 (1993) 8240.
[23] G.L. Griffin and J.T. Yates, Jr., J. Chem Phys., 77 (1982) 3782; 77 (1982) 3744; 77 (1982) 3751.
[24] J.C. Lavalley, J. Saissey and T. Rais, J. Mol. Catal., 17 (1982) 289.
[25] C. Chauvin, J. Saussey, J.C. Lavalley and G. Djega-Mariadasson, Appl. Catal., 25 (1986) 59.
[26] V. Bolis, B. Fubini, E. Giamello and A. Reller, J. Chem. Soc., Faraday Trans. 1, 85 (1989) 855.
[27] T.H. Ballinger and J.T. Yates Jr., Langmuir, 7 (1991) 3041.
[28] G. Busca, H. Saussey, O. Saur, J.C. Lavalley and V. Lorenzelli, Appl. Catal., 14 (1985) 245.
[29] G. Ramis, G. Busca and V. Lorenzelli, J. Chem. Soc., Faraday Trans. 1, 83 (1987) 1591.
[30] G. Oliveri, G. Ramis, G. Busca and V.S. Escribano, J. Mater. Chem., 3 (1993) 1239.
[31] P. Esser and W. Göpel, Surface Sci., 97 (1980) 309.
[32] W.T. Petrie and J.M. Vohs, Surface Sci. Lett., 259 (1991) L750.
[33] C.R. Henry, C. Chapon, C. Duriez and S. Giorgio, Surface Sci., 253 (1991) 177.
[34] C. Noda, H.H. Richardson and G.E. Ewing, J. Chem. Phys., 92 (1990) 2099.
[35] C. Noda and G.E. Ewing, Surface Sci., 240 (1990) 181; R. Disselkamp, H.-C. Chang and G.E. Ewing, Surface Sci., 240 (1990) 193.
[36] H.E. Sanders, P. Gardner, D.A. King and M.A. Morris, Surface Sci., 304 (1994) 159.
[37] F. Winkelmann, S. Wohlrab, J. Libuda, M. Bäumer, D. Cappus, M. Menges, K. Al-Shamery, H. Kuhlmbeck and H.-J. Freund, Surface Sci., 307–309 (1994) 1148.
[38] H.J. Freund, B. Dillmann, D. Ehrlich, M. Haßel, R.M. Jaeger, H. Kuhlenbeck, C.A. Ventrice Jr., F. Winkelmann, S. Wohlrab, C. Xu, Th. Bertrams, A. Brodde and H. Neddermeyer, J. Mol. Catal., 82 (1993) 143.
[39] H. Kuhlenbeck, C. Xu, B. Dillmann, M. Haßel, B. Adam, D. Ehrlich, S. Wohlrab, H.-J. Freund, U.A. Ditzinger, H. Neddermeyer, M. Neuber and M. Neumann, Ber. Bunsenges. Phys. Chem., 96(1) (1992) 15.
[40] H.-J. Freund and H. Kuhlenbeck, Springer Ser. Surface Sci., 35 (1994) 9.
[41] A. Freitag, V. Staemmler, D. Cappus, C.A. Ventrice Jr., K. Al Shamery, H. Kuhlenbeck and H.-J. Freund, Chem. Phys. Lett., 210(1/2/3) (1993) 10.
[42] F. Rohr, K. Wirth, J. Libuda, D. Cappus, M. Bäumer and H.-J. Freund, Surface Sci., 315 (1994) L977.
[43] D. Cappus, C. Xu, D. Ehrlich, B. Dillmann, C.A. Ventrice Jr., K. Al Shamery, H. Kuhlenbeck and H.-J. Freund, Chem. Phys., 177 (1993) 533.
[44] R.M. Jaeger, J. Libuda, M. Bäumer, K. Homann, H. Kuhlenbeck and H.-J. Freund, J. of Elect. Spectrosc., 64/65 (1993) 217.
[45] M. Bender, K. Al-Shamery and H.-J. Freund, Langmuir, 10(9) (1994) 3081.
[46] L.-J. Meng, C.P. Moreira de Sá and M.P. dos Santos, Appl. Surface Sci., 78 (1994) 57.
[47] M.L. Burke and D.W. Goodman, Surface Sci., 311 (1994) 17.
[48] J. Yoshinobu, T.H. Ballinger, Z. Xu, H.J. Jänsch, M.I. Zaki, J. Xu and J.T. Yates Jr., Surface Sci., 255 (1991) 295.
[49] R.M. Jaeger, H. Kuhlenbeck, H.-J. Freund, M, Wutting, W. Hoffmann, R. Franchy and H. Ibach, Surface Sci., 259 (1991) 235.
[50] F. Jensen, F. Besenbacher, E. Lægsgaard and I. Stensgaard, Surface Sci. Lett., 259 (1991) L774.
[51] N. Floquet and O. Bertrand, Surface Sci., 251/252 (1991) 1044.
[52] B.G. Frederick, G. Apai and T.N. Rhodin, Surface Sci., 244 (1991) 67.
[53] H. Schlienz, M. Beckendorf, U.J. Katter, T. Risse and H.-J. Freund, Phys. Rev. Lett., 74 (1995) 761.
[54] E. Escalona Platero, D. Scarano, G. Spoto and A. Zecchina, Faraday Discuss. Chem. Soc., 80 (1985) 183.
[55] A. Zecchina, S. Coluccia, G. Spoto, D. Scarano and L. Marchese, J. Chem. Soc., Faraday Trans., 86(4) (1990) 703.
[56] S. Coluccia, M. Baricco, L. Marchese, G. Martra and A. Zecchina, Spectrochim. Acta, 49A(9) (1993) 1289.
[57] L. Marchese, S. Coluccia, G. Martra and A. Zecchina, Surface Sci., 269/270 (1992) 135.
[58] E. Escalona Platero, S. Coluccia and A. Zecchina, Langmuir, 1 (1985) 407.
[59] E. Escalona Platero, B. Fubini and A. Zecchina, Surface Sci., 179 (1987) 404.
[60] E. Escalona Platero, S. Coluccia and A. Zecchina, Surface Sci., 171 (1986) 465.
[61] E. Escalona Platero, E. Garrone, G. Spoto and A. Zecchina, in Structure and Reactivity of Surfaces, Elsevier, Amsterdam, 1989, p. 395.
[62] E. Escalona Platero, G. Spoto, S. Coluccia and A. Zecchina, Langmuir, 3 (1987) 291.
[63] E. Escalona Platero et al., submitted for publication to Surface Science.
[64] A. Zecchina, G. Spoto, S. Coluccia and E. Guglielminotti, J. Chem. Soc., Faraday Trans. 1, 80 (1984) 1875.
[65] E. Escalona Platero, G. Spoto and A. Zecchina, J. Chem. Soc., Faraday Trans. 1, 81 (1985) 1283.
[66] D. Scarano, G. Spoto, S. Bordiga, S. Coluccia and A. Zecchina, J. Chem. Soc., Faraday Trans., 88(3) (1992) 291.
[67] A. Zecchina and F.S. Stone, J. Chem. Soc., Chem. Commun., (1974) 582.
[68] A. Zecchina and F.S. Stone, J. Chem. Soc., Faraday Trans. 1, 74 (1978) 2278.
[69] A. Zecchina, M.G. Lofthouse and F.S. Stone, J. Chem. Soc., Faraday Trans. 1, 71 (1975) 1476.
[70] E. Garrone, A. Zecchina and F.S. Stone, Philos. Mag. Sect. B, 42 (1980) 683.
[71] A. Zecchina, G. Spoto, S. Coluccia and E. Guglielminotti, J. Phys. Chem., 88 (1984) 2575; A. Zecchina, G. Spoto, E. Borello and E. Giamello, J. Phys. Chem., 88 (1984) 2582; A. Zecchina, G. Spoto, E. Garrone and A. Bossi, J. Phys. Chem., 88 (1984) 2587.

[72] A. Zecchina, G. Spoto, S. Coluccia and E. Garrone, J. Chem. Phys., 80(1) (1984) 467.
[73] E. Giamello, E. Garrone, S. Coluccia, G. Spoto and A. Zecchina, in G. Centi and F. Trifirò (Editors), New Developments in Selective Oxidation, Elsevier, Amsterdam, 1990, p. 817.
[74] A. Zecchina, G. Spoto and S. Coluccia, J. Mol. Catal., 14 (1982) 351.
[75] G. Ghiotti, A. Chiorino and F. Boccuzzi, Surface Sci., 287/288 (1993) 228.
[76] D. Scarano, G. Spoto and A. Zecchina, Surface Sci., 211/212 (1989) 1012.
[77] D. Scarano, G. Spoto, S. Bordiga and A. Zecchina, Surface Sci., 176 (1992) 281.
[78] F. Boccuzzi, C. Morterra, R. Scala and A. Zecchina, J. Chem. Soc., Faraday Trans. 2, 77 (1981) 2059.
[79] G. Hussain, M.M. Rahman and N. Sheppard, Can. J. Spectrosc., 33 (1988) 138.
[80] D. Scarano, A. Zecchina, G. Spoto and F. Geobaldo, submitted for publication to J. Chem. Soc., Faraday Trans., 1995.
[81] D. Scarano and A. Zecchina, Spectrochim. Acta, 43A(12) (1987) 1441.
[82] D. Scarano, A. Zecchina and A. Reller, Surface Sci., 198 (1988) 11.
[83] E. Escalona Platero, C. Otero Areán, D. Scarano, G. Spoto and A. Zecchina, Mater. Chem. Phys., 29 (1991) 347.
[84] D. Scarano, A. Zecchina, S. Bordiga, G. Ricchiardi and G. Spoto, Chem. Phys., 177 (1993) 547.
[85] D. Scarano, G. Spoto, S. Bordiga, G. Ricchiardi and A. Zecchina, J. Elect. Spectr. Rel. Phenom., 64/65 (1993) 307.
[86] D. Scarano, G. Spoto, S. Bordiga, L. Carnelli, G. Ricchiardi and A. Zecchina, Langmuir, 10 (1994) 3094.
[87] C. Morterra, G. Magnacca and N. Del Favero, Langmuir, 9 (1993) 642.
[88] A. Zecchina, E. Escalona Platero and C. Otero Areán, J. Catal., 107 (1987) 244.
[89] L. Marchese, S. Bordiga, S. Coluccia, G. Martra and A. Zecchina, J. Chem. Soc., Faraday Trans., 89(18) (1993) 3483.
[90] G. Spoto, C. Morterra, L. Marchese, L. Orio and A. Zecchina, Vacuum, 41(1–3) (1990) 37.
[91] C. Morterra, E. Garrone, V. Bolis and B. Fubini, Spectrochim. Acta, 43A(12) (1987) 1577.
[92] G. Cerrato, L. Marchese and C. Morterra, Appl. Surface Sci., 70/71 (1993) 200.
[93] C. Morterra, L. Orio, V. Bolis and P. Ugliengo, Mater. Chem. Phys., 29 (1991) 457.
[94] C. Morterra, V. Bolis, B. Fubini, L. Orio and T.B. Williams, Surface Sci., 251/252 (1991) 540.
[95] R. Larrson, R. Lykvist and B. Rebenstorf, Z. Phys. Chem., 263 (1982) 6.
[96] D.A. Dixon, J.L. Gole and A. Komornicki, J. Phys. Chem., 92 (1988) 1378.
[97] R.H. Hauge, S.E. Gransden and J.L. Margrave, J. Chem. Soc., Dalton Trans., (1979) 745.
[98] N.S. Hush and M.L. Williams, J. Mol. Spectrosc., 50 (1974) 349.
[99] G. Pacchioni, G. Cogliandro and P.S. Bagus, Surface Sci., 255 (1991) 344.
[100] K.M. Neyman and N. Rösch, Chem. Phys., 177 (1993) 561.
[101] K.M. Neyman and N. Rösch, Ber. Bunsenges. Phys. Chem., 96(11) (1992) 1711.
[102] R.A. Hammaker, S.A. Francis and R.P. Eischens, Spectrochim. Acta, 21 (1965) 1295.
[103] G.D. Mahan and A.A. Lucas, J. Chem. Phys., 68 (1978) 1344.
[104] B.N.J. Persson and R. Ryberg, Phys. Rev. B, 24 (1981) 6954.
[105] F.M. Hoffmann, Surface Sci. Reports, 3 (1983) 107.
[106] V.M. Browne, S.G. Fox and P. Hollins, Catal. Today, 9 (1991) 1.
[107] A. Crosseley and D.A. King, Surface Sci., 68 (1977) 528.
[108] D.P. Woodruff, B.E. Hayden, K. Prince and A.M. Bradshaw, Surface Sci., 123 (1982) 397.
[109] E.A. Culbourn, Surface Sci. Rep., 15 (1992) 281.
[110] P.W. Tasker, Phil. Mag. A, 39 (1979) 119.
[111] D.A., Seanor and C.H. Amberg, J. of Chem. Phys., 42(8) (1965) 2967.
[112] V. Bolis, B. Fubini, E. Garrone and C. Morterra, J. Chem. Soc., Farad. Trans. 1, 85 (1989) 1383.
[113] P.S. Braterman, in Metal Carbonyl Spectra, Academic Press, London, 1975, p. 177.
[114] S.F.A. Kettle and I. Paul, in F.G.A. Stone and R. West (Editors) Advances in Organometallic Chemistry, Vol. 10, Academic Press, New York, 1972, p. 199.
[115] J.W. Gadzuk, in J.T. Yates, Jr. and T.E. Madey (Editors) Vibrational Spectroscopy of Molecules on Surfaces, Plenum, New York, 1987.
[116] R.P.H. Gasser, in An Introduction to Chemisorption and Catalysis by Metals, Clarendon Press, Oxford, 1985.
[117] S.-S. Sung and R. Hoffmann, J. Am. Chem. Soc., 107 (1985) 578.
[118] C.V. Bauschlicher, Jr., P.S. Bagus, C.J. Nelin and B.O. Roos, J. Chem. Phys., 85(1) (1986) 354.
[119] C.V. Bauschlicher, Jr. and P.S. Bagus, J. Chem. Phys., 81(12) (1984) 5889.
[120] A. Mavridis, J.F. Harrison and J. Allison, J. Am. Chem. Soc., 111 (1989) 2482.
[121] C.T. Au, W. Hirsch and W. Hirschwald, Surface Sci., 197 (1988) 391.
[122] W. Göpel, R.S. Bauer and G. Hansson, Surface Sci., 99 (1980) 138.
[123] R.R. Gay, M.H. Nodine, V.E. Henrich, H.J. Zeiger and E.I. Solomon, J. Am. Chem. Soc., 102 (1980) 6752.
[124] A.B. Anderson and J.A. Nichols, J. Am. Chem. Soc., 108 (1986) 1385.
[125] J. Saillard and R. Hoffman, J. Am. Chem. Soc., 106 (1984) 2006.
[126] N.S. Hush and R.J.M. Hobbs in S.J. Lippard (Editor), Progress in Inorganic Chemistry, Vol. 10, Willey, New York, 1968, p. 379.
[127] V.M. Allen, W.E. Jones and P.D. Pacey, Surface Sci., 220 (1989) 193.
[128] P. Hollins, Surface Sci. Rep., 16 (1992) 51.
[129] M.I. Zaki and H. Knözinger, J. of Catalysis, 119 (1989) 311.

[130] M.I. Zaki and H. Knözinger, Spectrochim. Acta, 43A(12) (1987) 1455.
[131] D.H. Gay and A.L. Rohl, J. Chem. Soc., Faraday Trans., 91(5) (1995) 925.
[132] S. Blonski and S.H. Garofalini, Surface Sci., 295 (1993) 263.
[133] P. Hartmän, J. Cryst. Growth, 96 (1989) 667.
[134] H.E. Curry-Hyde, H. Munsch, A. Baiker, M. Schraml-Marth and A. Wokaun, J. Catal., 133 (1992) 397; M. Schraml-Marth, A. Wokaun and A. Baiker, J. Catal., 138 (1992) 306.
[135] A. Zecchina, D. Scarano and A. Reller, J. Chem. Soc., Faraday Trans. 1, 84(7) (1988) 2327.
[136] M. Causà, R. Dovesi, C. Pisani and C. Roetti, Surface Sci., 215 (1989) 259.
[137] F.H. Streitz and J.W. Mintmine, Phys. Rev. B, 50 (1994) 11996.
[138] G. Busca, V. Lorenzelli, G. Ramis and R.J. Willey, Langmuir, 9 (1993) 1492.
[139] G. Busca, P.F. Rossi, V. Lorenzelli, M. Benaisse, J. Travert and J.C. Lavalley, J. Phys. Chem., 89 (1989) 433.
[140] M.J. Davies, S.C. Parker and G.W. Watson, J. Mater. Chem., 4(6) (1994) 813.
[141] A.A. Tsyganenko, L.A. Denisenko, S.M. Zverev and V.N. Filimonov, J. Catal., 94 (1985) 10.
[142] L.A Denisenko, A.A. Tsyganenko and V.N. Filimonov, React. Kinet. Catal. Lett., 25 (1984) 23.